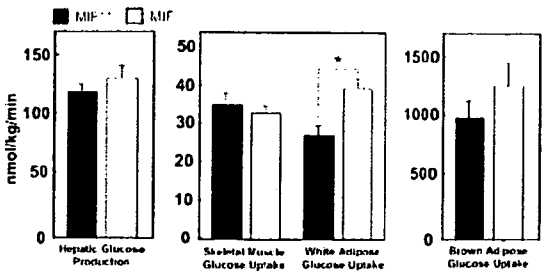

FIGURE 2. In vivo glucose metabolism in endotoxemic $MIF^{-/-}$ and $MIF^{+/+}$ mice. Seven to eight mice per group were pretreated with LPS, and organ-specific glucose metabolism was measured using labeled glucose in awake mice as described in the *Materials and Methods*. *, $p < 0.03$.

(16). The excess stain was removed and the cells were washed several times with water before microscopic examination and color quantification by NIH Image Analysis software.

Statistical analysis

Data are presented as mean ± SD. The statistical comparisons between groups were conducted using Student's t test. Values for $p < 0.05$ were considered significant.

Results

$MIF^{-/-}$ mice have an altered glycemic and plasma lactate response to endotoxin

Gram-negative endotoxin (LPS) is a powerful stimulus for the release of TNF-α and other proinflammatory cytokines, and LPS induces an acute hypoglycemic response when administered to experimental animals or human subjects (17). Prior studies using a neutralizing Ab approach demonstrated that anti-MIF inhibits the characteristic development of hypoglycemia in LPS-injected mice (5). We sought to verify these findings by administering a sublethal dose of LPS (16.6 μg/g) to $MIF^{-/-}$ mice and WT controls ($MIF^{+/+}$), and sampling their blood for measuring plasma glucose and lactate levels. $MIF^{-/-}$ mice showed a preservation of their glycemic and plasma lactate responses when compared with the WT mice (Fig. 1*A*). These differences were transient but most evident for lactate at 1.5 h and glucose at 2.5 h, which reflects the time necessary for systemic production of proinflammatory cytokines such as TNF-α and MIF (18). Plasma glucose levels were markedly lower (at 2.5 and 3 h), and plasma lactate levels were correspondingly higher (at 1.5 and 2 h) in the $MIF^{+/+}$ mice than in the $MIF^{-/-}$ mice. Although MIF has been shown to influence β-cell function (19), we observed no significant changes in plasma insulin levels, either at baseline (data not shown) or after LPS (2.5 h: $MIF^{+/+}$, 79 ± 12 pM, $MIF^{-/-}$, 69 ± 11 pM, p = NS; n = 5 mice per group). We also measured serum corticosterone, which may mediate increased glycemia as part of a systemic stress response. Notably, $MIF^{-/-}$ mice showed a decrease in circulating corticosterone levels when compared with $MIF^{+/+}$ mice, suggesting that glucocorticoids did not account for the increase in blood sugar during MIF deficiency (2.5 h: $MIF^{+/+}$, 0.42 ± 0.07 μM, $MIF^{-/-}$, 0.16 ± 0.04 μM, $p < 0.05$). There also were no differences in $MIF^{+/+}$ vs $MIF^{-/-}$ mice in circulating adiponectin, TNF-α, or

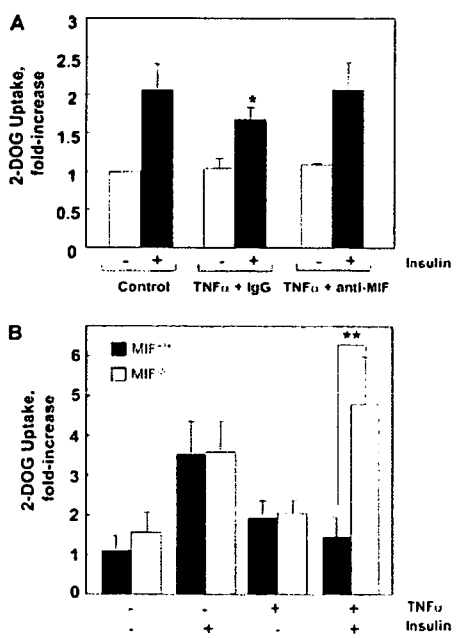

FIGURE 3. TNF-α has stimulatory action in glucose uptake into adipocytes. *A*, MIF neutralization reverses TNF-α-mediated reduction in adipocyte glucose transport. Cultured WT adipocytes were treated with TNF-α (20 ng/ml) together with an anti-MIF mAb or isotype control (each at 80 μg/ml). Basal and insulin-stimulated (100 nM, 5 min) uptake of 2-deoxyglucose (2-DOG) were performed as described in *Materials and Methods*. *B*, Primary mouse adipocytes were prepared from $MIF^{-/-}$ and $MIF^{+/+}$ mice and incubated overnight with or without TNF-α (20 ng/ml) for glucose transport studies. Data are means ± SD (n = 4 cultures). Data shown are representative of three independent experiments. *, $p < 0.05$ vs control; **, $p < 0.005$.

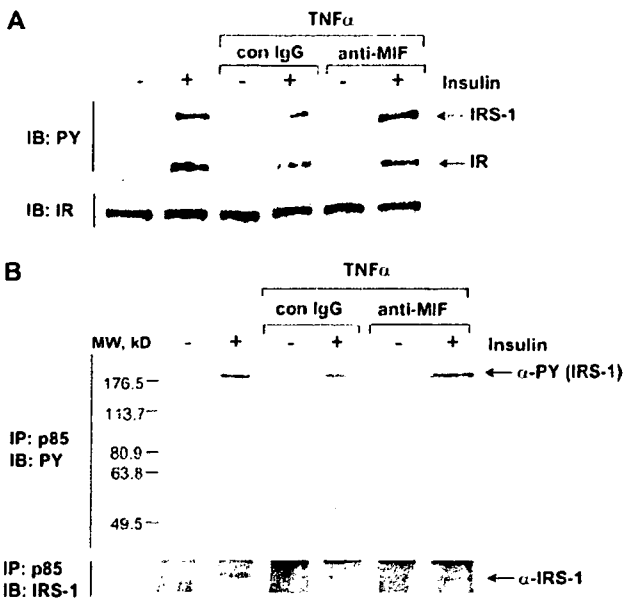

FIGURE 4. TNF-α action on the signal transduction events of the insulin receptor. *A*, Anti-MIF reduces TNF-α inhibition of the phosphorylation of IRS-1. 3T3-L1 adipocytes were stimulated with 20 ng/ml TNF-α for 6 h together with anti-MIF mAb or an isotypic control (IgG1) (each at 80 μg/ml) followed by stimulation with insulin (100 nM, 5 min). Cells were lysed, and Western blot analysis was performed with an anti-phosphotyrosine Ab (α-PY). The blots were stripped and reprobed with an insulin receptor-specific Ab (α-IRS-1). *B*, Anti-MIF mAb reduces the TNF-α-mediated decrease in the association of IRS-1 and PI3K subunit, p85. Cultured 3T3-L1 adipocytes were treated with 20 ng/ml TNF-α for 6 h together with anti-MIF mAb or an isotype control (each at 80 μg/ml), followed by stimulation with 100 nM insulin for 5 min. Whole cell lysates were immunoprecipitated with an anti-p85 Ab followed by Western blot analysis with an anti-phosphotyrosine Ab (α-PY). The blots were stripped and reprobed with an anti-IRS-1 Ab (α-IRS-1).

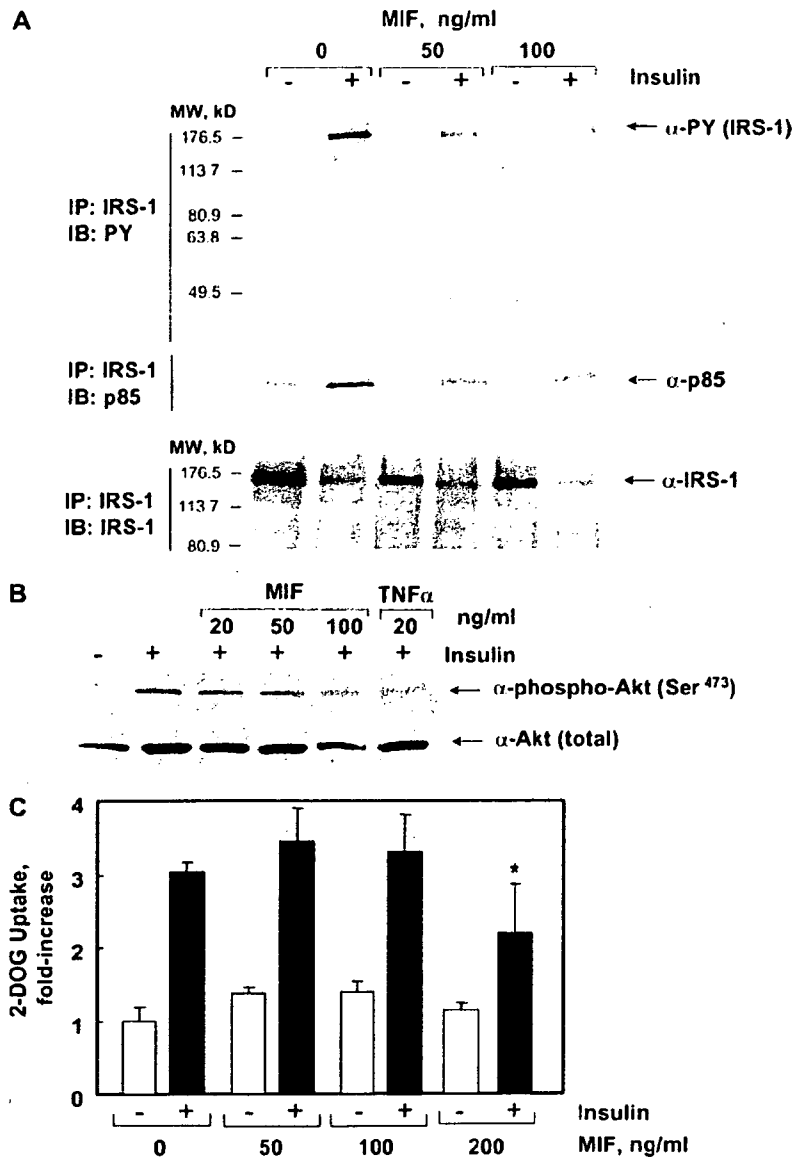

FIGURE 5. MIF-induced action on insulin signal transduction in adipocytes. *A*, MIF inhibits the insulin-induced tyrosine phosphorylation of IRS-1. Adipocytes were treated with increasing concentrations of recombinant MIF followed by insulin (100 nM) for 5 min. Immunoprecipitates were prepared from whole cell lysates using an anti-IRS-1 Ab followed by blotting analysis with anti-phosphotyrosine Ab (α-PY) (see *Materials and Methods*). The membrane was stripped and then reprobed with an anti-p85 Ab (α-p85) or an anti-IRS-1 Ab (α-IRS-1). *B*, MIF inhibits insulin-mediated phosphorylation of Akt. Cultured adipocytes were pretreated with MIF followed by insulin (100 nM) for 10 min. Total cell lysates were separated by SDS-PAGE and blotted with Abs against Ser^{473} phospho-Akt (α-phospho-Akt) and total Akt (αAkt). *C*, MIF decreases insulin-mediated 2-deoxyglucose (2-DOG) uptake in cultured adipocytes. Basal and insulin-stimulated uptake of 2-deoxyglucose into adipocytes was analyzed as described in *Materials and Methods*. Results were obtained in triplicate wells. Data shown (mean ± SD) are representative of three independently performed experiments. *, $p < 0.05$ vs control.

IL-6 levels, either at baseline (data not shown) or 2.5 h after LPS (adiponectin: $MIF^{+/+}$, 3.9 ± 0.3 ng/ml, $MIF^{-/-}$, 3.5 ± 0.3 ng/ml, p = NS; TNF-α: $MIF^{+/+}$, 57.0 ± 13.3 ng/ml, $MIF^{-/-}$, 69.6 ± 15.3 ng/ml, p = NS; and IL-6: $MIF^{+/+}$, 310 ± 100 ng/ml, $MIF^{-/-}$, 340 ± 80 ng/ml, p = NS). These genetically based results support an important role for MIF in the dysregulation of carbohydrate metabolism that occurs during endotoxemia.

Certain aspects of the metabolic effects of LPS can be recapitulated by the administration of TNF-α (4). To provide evidence for an effector role for MIF in the action of TNF-α, we next examined circulating glucose levels in $MIF^{-/-}$ and WT mice treated with a single, i.p. dose of TNF-α (160 μg/kg). TNF-α caused a marked reduction of blood glucose level in the WT mice, which is in agreement with prior reports (5, 17), and this effect occurred at least 1 h earlier than in mice administered LPS, which is in accord with the time delay necessary for TNF-α transcription, translation, and secretion. By contrast, $MIF^{-/-}$ mice treated with TNF-α were euglycemic in the acute phase (≤2 h), but then showed a reduction in blood glucose levels after 2 h (Fig. 1*B*). These data are in agreement with a prior report that anti-MIF may prevent TNF-α-induced hypoglycemia (5). The acute phase changes also are consistent with experiments supporting an MIF release response by cells and tissues exposed to TNF-α (5), and the reduction in blood glucose after 2 h may reflect a TNF-α-mediated induction of additional, downstream mediators (1).

Glucose uptake into adipose tissue is increased in endotoxemic, $MIF^{-/-}$ mice

To better assess the impact of MIF deficiency on glucose metabolism during endotoxemia, we measured organ-specific glucose uptake in awake mice at 2.5 h following sublethal treatment with LPS. Hepatic glucose production and glucose uptake into skeletal muscle (gastrocnemius) and adipose tissues were determined using continuous infusion of 3-[^{3}H]glucose and a bolus injection of 2-[^{14}C]DG as a nonmetabolizable glucose analog. As shown in Fig. 2, MIF deficiency was associated with a significant and selective increase in glucose uptake into white adipose tissue. In contrast, glucose uptake in skeletal muscle and brown adipose tissue, and hepatic glucose production were not significantly affected under these experimental conditions.

The inhibitory action of TNF-α on insulin-mediated glucose transport is reversed by MIF immunoneutralization or genetic deficiency

The preceding observations, together with the report that TNF-α-treated adipocytes secrete MIF (9), prompted us to examine the role of MIF in mediating the effect of TNF-α on adipocyte glucose metabolism. We verified that TNF-α (2 ng/ml) induced MIF secretion from cultured adipocytes, and we observed a diminution in MIF release at very high TNF-α concentrations (≥20 ng/ml), which is in agreement with prior observations in TNF-α-treated monocytes/macrophages (6 and data not shown).

TNF-α inhibits the stimulatory action of insulin on glucose uptake into adipocytes (20). We treated adipocytes with TNF-α and measured insulin-stimulated uptake of 2-deoxyglucose in the presence of anti-MIF mAb or an isotypic, IgG1 control. The insulin-stimulated uptake of 2-deoxyglucose was significantly greater upon MIF immunoneutralization (Fig. 3*A*). The inhibitory action of MIF upon 2-deoxyglucose uptake was verified in studies performed in primary adipocytes isolated from $MIF^{-/-}$ mice. As shown in Fig. 3*B*, adipocytes genetically deficient in MIF showed a significant increase in 2-deoxyglucose uptake despite treatment with TNF-α. These data support a model whereby TNF-α inhibits insulin signal transduction via the autocrine/paracrine secretion of MIF. Such a mechanism of TNF-α action also is consistent with studies in differentiated myotubes, where TNF-α was found to induce MIF release, leading to a downstream, autocrine/paracrine response (5).

Immunoneutralization of MIF reverses TNF-α-mediated insulin resistance in cultured adipocytes

A well-characterized action of TNF-α with respect to glucose transport is inhibition of insulin signal transduction leading to insulin resistance (21). We followed a standard protocol for inducing insulin resistance in vitro and treated adipocytes with TNF-α together with a neutralizing anti-MIF mAb or isotype control, followed by stimulation with insulin for 5 min. As expected, insulin induced the rapid tyrosine phosphorylation of the insulin receptor and the IRS-1, and these events were inhibited by TNF-α pretreatment (Fig. 4*A*). The addition of anti-MIF mAb, but not control Ab, significantly reduced the action of TNF-α on the tyrosine phosphorylation of the insulin receptor and IRS-1.

The enzyme PI3K is a downstream mediator of insulin signal transduction, and it plays an important role in the insulin-dependent translocation of GLUT4 (22). PI3K is comprised of a 110-kDa catalytic subunit and an 85-kDa regulatory subunit with Src homology 2 domains that bind to the tyrosine-phosphorylated isoform of IRS-1. The functional significance of the TNF-α-dependent reduction in IRS-1 tyrosine phosphorylation can be monitored by coimmunoprecipitation of the IRS-1 complex containing the p85 regulatory subunit of PI3K (23). We examined the effect of MIF neutralization on the TNF-α-mediated decrease in the association of IRS-1 and PI3K (p85). As shown in Fig. 4*B*, the insulin-induced association of IRS-1 with PI3K (p85 subunit) was reduced by TNF-α treatment, and anti-MIF inhibited this specific action of TNF-α on adipocytes. These data, taken together, are consistent with a role for MIF in mediating the action of TNF-α on the proximal signal transduction events induced by insulin receptor ligation.

Recombinant MIF inhibits insulin signal transduction in adipocytes

To provide a more direct assessment of MIF action on adipocytes, we treated cells with different concentrations of MIF before stimulation by insulin. As shown in Fig. 5*A*, exogenously added MIF decreased the tyrosine phosphorylation of IRS-1 as well as the insulin-induced association of IRS-1 with the p85 regulatory subunit of PI3K. This effect occurred in a dose-dependent fashion, and at concentrations of MIF that are within the range for those reported in patients with sepsis or severe inflammation (7, 8). The serine-threonine kinase Akt is a downstream target of PI3K (24) that is recruited to the membrane by PI3K-generated phospholipids. Akt undergoes phosphorylation and activation, and provides signals for the synthesis of new glucose transporters and enhanced glucose uptake. We examined the effect of exogenously added MIF on insulin-mediated, Ser^{473} phosphorylation of Akt in adipocytes. Cells were treated with MIF followed by insulin (100 nM) for 10 min. As shown in Fig. 5*B*, MIF inhibited the insulin-induced phosphorylation of Akt.

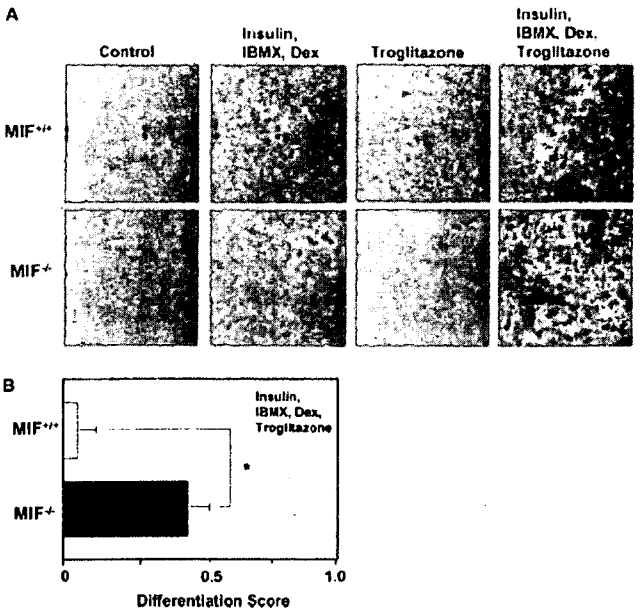

FIGURE 6. MIF deficiency enhances adipocyte differentiation. *A*, MEFs were prepared from $MIF^{+/+}$ or $MIF^{-/-}$ mice, and differentiation into adipocytes induced as shown. Differentiation was assessed visually by staining with Oil red O at a magnification of ×100. *B*, Quantification of color intensity by NIH Image Analyzer software is shown. Data are representative of four experiments each performed with independently derived fibroblast cell lines. *, $p < 0.001$.

Next, we investigated the action of MIF on basal and insulin-mediated glucose uptake. The addition of MIF to adipocytes did not cause an appreciable change in basal 2-deoxyglucose uptake (Fig. 5*C*). A decrease in insulin-stimulated glucose uptake was observed in this cultured cell system at 200 ng/ml MIF. These data differ from those reported in differentiated myotubes, where MIF was found to augment basal glucose uptake and not to influence insulin-mediated glucose uptake (5). This difference in response likely reflects the selective use of insulin-sensitive vs insensitive glucose transporters in these two differentiated cell types (25).

Genetic deficiency in MIF increases adipogenesis

We next examined the influence of MIF in adipogenesis, which is known to be inhibited by TNF-α (26). We prepared embryonic fibroblasts from $MIF^{+/+}$ and $MIF^{-/-}$ mice and subjected them to defined adipocyte differentiation protocols (27). We found that although $MIF^{-/-}$ cells responded similarly to $MIF^{+/+}$ cells when exposed to a standard differentiation medium (insulin, isobutylmethylxanthine, and dexamethasone) or to the peroxisome proliferator-activated receptor (PPAR)γ agonist, troglitazone, the

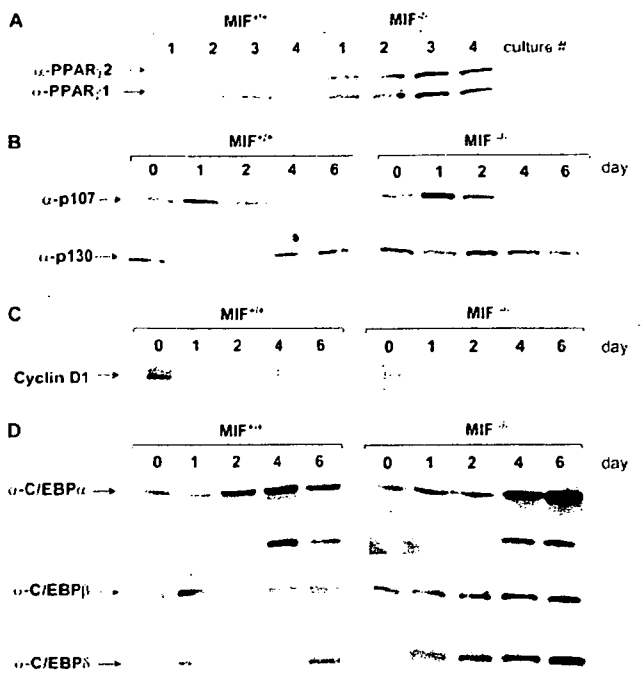

FIGURE 7. Impact of MIF deficiency on signaling pathways associated with adipogenesis. *A*, The expression of PPARγ proteins after induction of adipogenesis. Cells were grown in standard differentiation medium in the presence of troglitazone and harvested at day 9. The Western blot analysis of lysates from cultures of four different MEF cell lines (*lanes 1–4*) is shown. *B*, The expression of the p107 and p130 transcriptional regulatory proteins during adipocyte differentiation. $MIF^{+/+}$ and $MIF^{-/-}$ MEFs were grown in standard differentiation medium in the presence of troglitazone and harvested at the indicated days for Western blot analysis with anti-p107 (α-p107) or anti-p130 (α-p130) Ab. *C*, The expression of cyclin D1 protein during adipocyte differentiation. $MIF^{+/+}$ and $MIF^{-/-}$ MEFs were grown in standard differentiation medium in the presence of troglitazone and analyzed by Western blotting with anti-cyclin D1 Ab. *D*, The expression of C/EBPα, C/EBPβ, and C/EBPδ proteins during adipogenesis. Cells were grown as described, harvested on the indicated days, and Western blot analyzed with the C/EBP-specific Abs shown. The blot for C/EBPα shows both the p42 and the p30 isoforms.

$MIF^{-/-}$ cells were significantly more sensitive to the combination of standard differentiation medium plus troglitazone (Fig. 6). Adipocyte differentiation is known to be linked to the transcriptional activation of the PPARγ, which is a target for the differentiation agent, troglitazone. We observed higher expression of the PPARγ1 and PPARγ2 isoforms during differentiation of the $MIF^{-/-}$ cells vs the $MIF^{+/+}$ cells (Fig. 7*A*). Fibroblasts exposed to adipogenic factors enter a stage of postconfluent, cell division that is associated with a switch in the expression of the p130:p107 transcriptional regulatory proteins (28). We analyzed the expression of p130:p107 during adipocyte differentiation and found a similar pattern of expression in both the $MIF^{-/-}$ and $MIF^{+/+}$ cells (Fig. 7*B*). The expression of cyclin D1 and the subsequent activation of cyclin-dependent kinases has been shown to inhibit adipocyte differentiation (38). We analyzed cyclin D1 levels by western blotting and observed the expected down-regulation of this protein after the addition of differentiation medium to $MIF^{+/+}$ cells. By contrast, the expression of cyclin D1 was significantly reduced at baseline in $MIF^{-/-}$ cells, which appears consonant with the increased sensitivity of these cells to adipocyte differentiation (Fig. 7*C*).

Finally, we examined the expression of C/EBPα, C/EBPβ, and C/EBPδ, which are transcriptionally activated during adipogenesis.

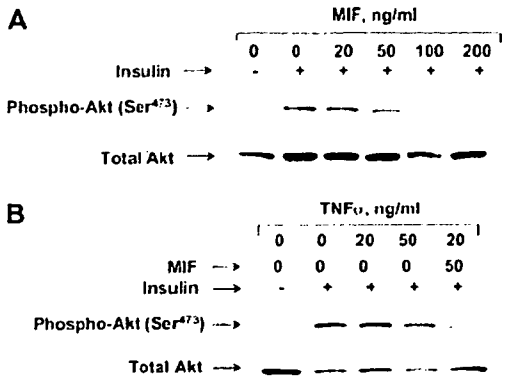

FIGURE 8. The effect of MIF or TNF-α on the insulin-mediated phosphorylation of Akt in $MIF^{-/-}$ adipocytes. *A*, Cultured adipocytes were pretreated with MIF for 6 h followed by insulin (100 nM) for 10 min. Total cell lysates were separated by SDS-PAGE and blotted with Abs against Ser^{473} phospho-Akt and total Akt. *B*, Cultured adipocytes were pretreated with TNF-α, or TNF-α plus MIF, for 6 h followed by insulin (100 nM) for 10 min. Total cell lysates were separated by SDS-PAGE and blotted with Abs against Ser^{473} phospho-Akt and total Akt.

C/EBPβ and C/EBPδ are induced early and activate the expression of PPARγ, and C/EBPα is induced later in time (29). MIF deficiency was associated with an up-regulation of C/EBPα, C/EBPβ, and C/EBPδ during the six-day period of adipocyte differentiation (Fig. 7*D*). MIF-deficient cells thus show an increased ability to differentiate into adipocytes in response to PPARγ ligands, and this effect may result from a constitutive reduction in baseline cyclin D1 levels and an enhancement in cellular C/EBPα, C/EBPβ, and C/EBPδ content.

The effect of MIF or TNF-α on insulin-mediated phosphorylation of Akt in $MIF^{-/-}$ adipocytes

To further evaluate the functional phenotype of $MIF^{-/-}$ adipocytes, we examined the effect of MIF or TNF-α on insulin-mediated signal transduction in these cells. $MIF^{-/-}$ adipocytes were exposed to MIF or TNF-α and the insulin induced phosphorylation of Akt was analyzed by western blotting. As shown in Fig. 8, MIF inhibits the insulin-mediated phosphorylation of Akt, whereas TNF-α showed no significant effect. We also examined the presence of TNFRs during the differentiation of both $MIF^{-/-}$ and $MIF^{+/+}$ adipocytes, because a reduction in the TNFR could offer an explanation for the TNF insensitivity of $MIF^{-/-}$ cells. The expression of TNFR-1 protein was induced in equivalent levels in $MIF^{-/-}$ and $MIF^{+/+}$ cells, and no differences were noted in the expression of the TNFR-2 isoform (Fig. 9 and data not shown).

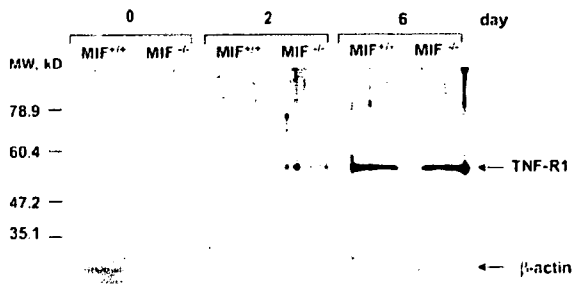

FIGURE 9. The expression of TNFR (TNF-R1) during adipocyte differentiation of $MIF^{+/+}$ and $MIF^{-/-}$ MEFs. Total cell lysates were separated by SDS-PAGE and blotted with Abs against TNFR-1 Ab. The blot was stripped and reprobed with anti-β-actin Ab.

Discussion

Investigations of the metabolic dysregulation that accompanies severe infection or tissue invasion led in the 1980s to the definition of the mediator "cachectin", which was later determined to be structurally identical with TNF-α (30). Among the metabolic changes noted in these studies were insulin resistance and alterations in glucose and lipid homeostasis that affected the rate of substrate production and use by tissues. There has been an accumulation of data supporting the importance of TNF-α in insulin resistance, both in acute disease and in conditions such as diabetes and obesity (3, 20, 21, 31). The importance of metabolic homeostasis to clinical outcome also has been highlighted by observations of decreased mortality in critically ill patients treated with insulin therapy (32).

MIF is an established mediator of sepsis lethality (7), and it is secreted by activated immune cells (6), by the anterior pituitary (10), and by the β-cells of the pancreatic islets, where it is a positive, autocrine regulator of insulin release (19). In a recent study, MIF was described to be released from cultured myotubes stimulated with TNF-α and then to act in an autocrine/paracrine manner to stimulate muscle glucose catabolism (5). In the present study, $MIF^{-/-}$ mice showed a near normalization in glucose metabolism in response to endotoxin, which induces a transient (<2 h) alteration in circulating glucose and lactate levels. Moreover, TNF-α itself did not influence blood glucose in the setting of genetic MIF deficiency. An intrinsic role of MIF in the glycemic response during endotoxemia was verified by in vivo experiments using labeled glucose in awake mice, which showed increased glucose uptake into white adipose tissue in mice genetically deficient in MIF. Anti-MIF mAb also prevented TNF-α inhibition of insulin-mediated glucose transport in adipocytes, which is in accord with a modulating effect of MIF on the action of TNF-α at the level of insulin signal transduction. The precise mechanism for the inhibitory effect of MIF on insulin signal transduction events may involve inhibition of Akt phosphorylation, which together with PI3K is necessary for the serine phosphorylation of the IRS-1 protein (23, 33).

Genetic MIF deficiency also promotes adipogenesis in a defined model of adipocyte differentiation requiring PPARγ agonism, and this effect is consistent with an inhibitory action of TNF-α on adipocyte differentiation (34). Among the mechanisms by which MIF may mediate this inhibition it is notable that the E2F family regulates the differentiation of adipocytes. E2F1 induces PPARγ transcription during clonal expansion (35), and Petrenko et al. (36) recently showed that the expression of E2F1 is up-regulated in $MIF^{-/-}$ cells. An additional pathway may relate to the defect in cyclin D1 activity that has been described in fibroblasts deficient in MIF (37). Fu et al. (38) have reported that cyclin D1 inhibits PPARγ-mediated adipogenesis via an action on histone deacetylase. $MIF^{-/-}$ cells showed reduced levels of cyclin D1, which is in agreement with the enhanced adipogenic potential of these cells. MIF also showed an inhibitory action on C/EBPδ. The C/EBPδ transcription factor is induced by the dexamethasone (39), and this action is likely consistent with the glucocorticoid counter-regulating properties of MIF (18, 40).

TNF-α did not affect the insulin-mediated phosphorylation of Akt in $MIF^{-/-}$ adipocytes, further confirming the role for MIF as a downstream effector of TNF-α. This effect was not due to reduced expression of TNFR-1 by these cells, which may be suggested by a prior report (42). It is known, however, that the action of TNF-α on insulin signaling is reduced upon PPARγ activation (41). Although we cannot rule out a role for MIF in affecting PPARγ activation, the PPARγ ligand troglitazone by itself did not show a differential effect on adipocyte development from $MIF^{+/+}$ vs $MIF^{-/-}$ cells. Further studies will be necessary to better define the signaling pathways influenced by the interaction of TNF-α and MIF in this model system.

In conclusion, these studies support the concept that TNF-α mediates insulin resistance in adipocytes by the downstream, autocrine/paracrine action of MIF on key steps in the insulin signal transduction pathway. The present studies nevertheless do not signify that all of the metabolic actions of TNF-α are necessarily attributed to MIF. A broader question regards the potential action of MIF in carbohydrate and lipid homeostasis in physiologic settings outside of severe inflammation. Patients who have type 2 diabetes have increased circulating levels of MIF (43, 44), and the recent discovery of functional alleles in the human *MIF* gene (45), prompt consideration of the role of MIF in the pathogenesis of insulin resistance that occurs more commonly in diabetes, aging, and obesity.

Disclosures

Drs. Leng, Metz, Mitchell, and Bucala are coinventors on patents describing the potential therapeutic value of inhibiting MIF.

References

1. Michie, H. R. 1996. Metabolism of sepsis and multiple organ failure. *World J. Surg.* 20: 460–464.
2. Khovidhunkit, W., M. S. Kim, R. A. Memon, J. K. Shigenaga, A. H. Moser, K. R. Feingold, and C. Grunfeld. 2004. Effects of infection and inflammation on lipid and lipoprotein metabolism: mechanisms and consequences to the host. *J. Lipid Res.* 45: 1169–1196.
3. Wellen, K. E., and G. S. Hotamisligil. 2005. Inflammation, stress, and diabetes. *J. Clin. Invest.* 115: 1111–1119.
4. Beutler, B., I. W. Milsark, and A. C. Cerami. 1985. Passive immunization against cachectin/tumor necrosis factor protects mice from lethal effect of endotoxin. *Science* 229: 869–871.
5. Benigni, F., T. Atsumi, T. Calandra, C. Metz, B. Echtenacher, T. Peng, and R. Bucala. 2000. The proinflammatory mediator macrophage migration inhibitory factor induces glucose catabolism in muscle. *J. Clin. Invest.* 106: 1291–1300.
6. Calandra, T., J. Bernhagen, R. A. Mitchell, and R. Bucala. 1994. The macrophage is an important and previously unrecognized source of macrophage migration inhibitory factor. *J. Exp. Med.* 179: 1895–1902.
7. Calandra, T., B. Echtenacher, D. L. Roy, J. Pugin, C. N. Metz, L. Hültner, D. Heumann, D. Männel, R. Bucala, and M. P. Glauser. 2000. Protection from septic shock by neutralization of macrophage migration inhibitory factor. *Nat. Med.* 6: 164–170.
8. Bozza, F. A., R. N. Gomes, A. M. Japiassú, M. Soares, H. C. Castro-Faria-Neto, P. T. Bozza, and M. T. Bozza. 2004. Macrophage migration inhibitory factor levels correlate with fatal outcome in sepsis. *Shock* 22: 309–313.
9. Hirokawa, J., S. Sakaue, S. Tagami, Y. Kawakami, M. Sakai, S. Nishi, and J. Nishihira. 1997. Identification of macrophage migration inhibitory factor in adipose tissue and its induction by tumor necrosis factor-α. *Biochem. Biophys. Res. Commun.* 235: 94–98.
10. Bernhagen, J., T. Calandra, R. A. Mitchell, S. B. Martin, K. J. Tracey, W. Voelter, K. R. Manogue, A. Cerami, and R. Bucala. 1993. MIF is a pituitary-derived cytokine that potentiates lethal endotoxaemia. *Nature* 365: 756–759.
11. Bozza, M., A. R. Satoskar, G. Lin, B. Lu, A. A. Humbles, C. Gerard, and J. R. David. 1999. Targeted disruption of migration inhibitory factor gene reveals its critical role in sepsis. *J. Exp. Med.* 189: 341–346.
12. Kim, J. K., J. J. Fillmore, O. Gavrilova, L. Chao, T. Higashimori, H. Choi, H. J. Kim, C. Yu, Y. Chen, X. Qu, et al. 2003. Differential effects of rosiglitazone on skeletal muscle and liver insulin resistance in A-ZIP/F-1 fatless mice. *Diabetes* 52: 1311–1318.
13. Bedard, S., B. Marcotte, and A. Marette. 1997. Cytokines modulate glucose transport in skeletal muscle by inducing the expression of inducible nitric oxide synthase. *Biochem. J.* 325(Pt. 2): 487–493.
14. Liu, Y. Q., K. Tornheim, and J. L. Leahy. 1998. Shared biochemical properties of glucotoxicity and lipotoxicity in islets decrease citrate synthase activity and increase phosphofructokinase activity. *Diabetes* 47: 1889–1893.
15. Fingerle-Rowson, G., O. Petrenko, C. N. Metz, T. G. Forsthuber, R. Mitchell, R. Huss, U. Moll, W. Müller, and R. Bucala. 2003. The p53-dependent effects of macrophage migration inhibitory factor revealed by gene targeting. *Proc. Natl. Acad. Sci. USA* 100: 9354–9359.
16. Sakaue, H., W. Ogawa, M. Matsumoto, S. Kuroda, M. Takata, T. Sugimoto, B. M. Spiegelman, and M. Kasuga. 1998. Posttranscriptional control of adipocyte differentiation through activation of phosphoinositide 3-kinase. *J. Biol. Chem.* 273: 28945–28952.
17. Evans, D. A., D. O. Jacobs, and D. W. Wilmore. 1989. Tumor necrosis factor enhances glucose uptake by peripheral tissues. *Am. J. Physiol.* 257: R1182–R1189.
18. Calandra, T., J. Bernhagen, C. N. Metz, L. A. Spiegel, M. Bacher, T. Donnelly, A. Cerami, and R. Bucala. 1995. MIF as a glucocorticoid-induced modulator of cytokine production. *Nature* 377: 68–71.

19. Waeber, G., T. Calandra, R. Roduit, J. A. Haefliger, C. Bonny, N. Thompson, B. Thorens, E. Temler, A. Meinhardt, M. Bacher, et al. 1997. Insulin secretion is regulated by the glucose-dependent production of islet beta cell macrophage migration inhibitory factor. *Proc. Natl. Acad. Sci. USA* 94: 4782–4787.
20. Hotamisligil, G. S., P. Arner, J. F. Caro, R. L. Atkinson, and B. M. Spiegelman. 1995. Increased adipose tissue expression of tumor necrosis factor-α in human obesity and insulin resistance. *J. Clin. Invest.* 95: 2409–2415.
21. Hotamisligil, G. S., D. L. Murray, L. N. Choy, and B. M. Spiegelman. 1994. Tumor necrosis factor α inhibits signaling from the insulin receptor. *Proc. Natl. Acad. Sci. USA* 91: 4854–4858.
22. Rordorf-Nikolic, T., D. J. Van Horn, D. Chen, M. F. White, and J. M. Backer. 1995. Regulation of phosphatidylinositol 3′-kinase by tyrosyl phosphoproteins: full activation requires occupancy of both SH2 domains in the 85-kDa regulatory subunit. *J. Biol. Chem.* 270: 3662–3666.
23. Kanety, H., R. Feinstein, M. Z. Papa, R. Hemi, and A. Karasik. 1995. Tumor necrosis factor alpha-induced phosphorylation of insulin receptor substrate-1 (IRS-1): possible mechanism for suppression of insulin-stimulated tyrosine phosphorylation of IRS-1. *J. Biol. Chem.* 270: 23780–23784.
24. Hill, M. M., S. F. Clark, D. F. Tucker, M. J. Birnbaum, D. E. James, and S. L. Macaulay. 1999. A role for protein kinase Bbeta/Akt2 in insulin-stimulated GLUT4 translocation in adipocytes. *Mol. Cell Biol.* 19: 7771–7781.
25. Mitsumoto, Y., and A. Klip. 1992. Development regulation of the subcellular distribution and glycosylation of GLUT1 and GLUT4 glucose transporters during myogenesis of L6 muscle cells. *J. Biol. Chem.* 267: 4957–4962.
26. Ninomiya-Tsuji, J., F. M. Torti, and G. M. Ringold. 1993. Tumor necrosis factor-induced *c-myc* expression in the absence of mitogenesis is associated with inhibition of adipocyte differentiation. *Proc. Natl. Acad. Sci. USA* 90: 9611–9615.
27. Rubin, C. S., A. Hirsch, C. Fung, and O. M. Rosen. 1978. Development of hormone receptors and hormonal responsiveness in vitro: insulin receptors and insulin sensitivity in the preadipocyte and adipocyte forms of 3T3-L1 cells. *J. Biol. Chem.* 253: 7570–7578.
28. Richon, V. M., R. E. Lyle, and R. E. McGehee, Jr. 1997. Regulation and expression of retinoblastoma proteins p107 and p130 during 3T3-L1 adipocyte differentiation. *J. Biol. Chem.* 272: 10117–10124.
29. Wu, Z., Y. Xie, N. L. Bucher, and S. R. Farmer. 1995. Conditional ectopic expression of C/EBPβ in NIH-3T3 cells induces PPARγ and stimulates adipogenesis. *Genes Dev.* 9: 2350–2363.
30. Beutler, B., J. Mahoney, N. Le Trang, P. Pekala, and A. Cerami. 1985. Purification of cachectin, a lipoprotein lipase-suppressing hormone secreted by endotoxin-induced RAW 264.7 cells. *J. Exp. Med.* 161: 984–995.
31. Hotamisligil, G. S., N. S. Shargill, and B. M. Spiegelman. 1993. Adipose expression of tumor necrosis factor-α: direct role in obesity-linked insulin resistance. *Science* 259: 87–91.
32. van den Berghe, G., P. Wouters, F. Weekers, C. Verwaest, F. Bruyninckx, M. Schetz, D. Vlasselaers, P. Ferdinande, P. Lauwers, and R. Bouillon. 2001. Intensive insulin therapy in the critically ill patients. *N. Engl. J. Med.* 345: 1359–1367.
33. Hotamisligil, G. S., P. Peraldi, A. Budavari, R. Ellis, M. F. White, and B. M. Spiegelman. 1996. IRS-1-mediated inhibition of insulin receptor tyrosine kinase activity in TNF-α- and obesity-induced insulin resistance. *Science* 271: 665–668.
34. Xu, H., J. K. Sethi, and G. S. Hotamisligil. 1999. Transmembrane tumor necrosis factor (TNF)-α inhibits adipocyte differentiation by selectively activating TNF receptor 1. *J. Biol. Chem.* 274: 26287–26295.
35. Fajas, L., R. L. Landsberg, Y. Huss-Garcia, C. Sardet, J. A. Lees, and J. Auwerx. 2002. E2Fs regulate adipocyte differentiation. *Dev. Cell* 3: 39–49.
36. Petrenko, O., G. Fingerle-Rowson, T. Peng, R. A. Mitchell, and C. N. Metz. 2003. Macrophage migration inhibitory factor deficiency is associated with altered cell growth and reduced susceptibility to Ras-mediated transformation. *J. Biol. Chem.* 278: 11078–11085.
37. Liao, H., R. Bucala, and R. A. Mitchell. 2003. Adhesion-dependent signaling by macrophage migration inhibitory factor (MIF). *J. Biol. Chem.* 278: 76–81.
38. Fu, M., M. Rao, T. Bouras, C. Wang, K. Wu, X. Zhang, Z. Li, T. P. Yao, and R. G. Pestell. 2005. Cyclin D1 inhibits peroxisome proliferator-activated receptor γ-mediated adipogenesis through histone deacetylase recruitment. *J. Biol. Chem.* 280: 16934–16941.
39. Cao, Z., R. M. Umek, and S. L. McKnight. 1991. Regulated expression of three C/EBP isoforms during adipose conversion of 3T3-L1 cells. *Genes Dev.* 5: 1538–1552.
40. Fingerle-Rowson, G., P. Koch, R. Bikoff, X. Lin, C. N. Metz, F. S. Dhabhar, A. Meinhardt, and R. Bucala. 2003. Regulation of macrophage migration inhibitory factor expression by glucocorticoids in vivo. *Am. J. Pathol.* 162: 47–56.
41. Iwata, M., T. Haruta, I. Usui, Y. Takata, A. Takano, T. Uno, J. Kawahara, E. Ueno, T. Sasaoka, O. Ishibashi, and M. Kobayashi. 2001. Pioglitazone ameliorates tumor necrosis factor-α-induced insulin resistance by a mechanism independent of adipogenic activity of peroxisome proliferator–activated receptor-γ. *Diabetes* 50: 1083–1092.
42. Toh, M. L., D. Aeberli, D. Lacey, Y. Yang, L. L. Santos, M. Clarkson, L. Sharma, C. Clyne, and E. F. Morand. 2006. Regulation of IL-1 and TNF receptor expression and function by endogenous macrophage migration inhibitory factor. *J. Immunol.* 177: 4818–4825.
43. Yabunaka, N., J. Nishihira, Y. Mizue, M. Tsuji, M. Kumagai, Y. Ohtsuka, M. Imamura, and M. Asaka. 2000. Elevated serum content of macrophage migration inhibitory factor in patients with type 2 diabetes. *Diabetes Care* 23: 256–258.
44. Vozarova, B., N. Stefan, R. Hanson, R. S. Lindsay, C. Bogardus, P. A. Tataranni, C. Metz, and R. Bucala. 2002. Plasma concentrations of macrophage migration inhibitory factor are elevated in Pima Indians compared to Caucasians and are associated with insulin resistance. *Diabetologia* 45: 1739–1741.
45. Gregersen, P. K., and R. Bucala. 2003. Macrophage migration inhibitory factor, MIF alleles, and the genetics of inflammatory disorders: incorporating disease outcome into the definition of phenotype. *Arthritis Rheum.* 48: 1171–1176.

ARTHRITIS & RHEUMATISM
Vol. 56, No. 8, August 2007, pp 2803–2809

CONCISE COMMUNICATIONS

DOI 10.1002/art.22799

A polymorphism in human platelet antigen 6b and risk of thrombocytopenia in patients with systemic lupus erythematosus

Systemic lupus erythematosus (SLE) is a systemic autoimmune disorder characterized by circulating autoantibodies directed against nuclear, cytoplasmic, cell membrane, and other autoantigens. Possible manifestations of SLE include the thrombocyte-associated diseases autoimmune thrombocytopenia and thrombosis.

The platelet surface glycoprotein IIb-IIIa (GPIIb-IIIa) complex plays an important role in platelet aggregation and hemostasis, since it is a receptor for fibrinogen, von Willebrand factor, and fibronectin. This complex constitutes a major target for antiplatelet antibodies responsible for immune-related thrombocytopenia (1).

GPIIIa is highly polymorphic, and 5 human platelet antigen (HPA) systems (HPA-1, HPA-4, HPA-6, HPA-7, and HPA-8) are known to be located in this glycoprotein. Polymorphisms in this region have been associated with neonatal alloimmune thrombocytopenia, posttransfusion purpura, and refractoriness to platelet transfusion in European American populations (2). Thus, these polymorphisms may be important as alloantigen determinants. In addition, evidence has been found to support a significant association between HPA-1 polymorphism and thrombosis (3,4), suggesting that HPA is involved in platelet aggregation.

In the Japanese population, polymorphisms in HPA-1, HPA-7, and HPA-8 are very rare. In a previous study, only 1 of 331 random donors was found to be A/B heterozygous in HPA-1, and no polymorphisms were detected in HPA-7 or HPA-8 in any of the subjects (5). The frequencies of polymorphisms in other HPA systems were 2.2% for A/B in HPA-4 and 5.1% for A/B and 0.3% for B/B in HPA-6 (5).

In the present study, we analyzed HPA-1, HPA-4, and HPA-6 polymorphisms in Japanese patients with SLE to determine the association of these polymorphisms with thrombocytopenia and thrombosis. A total of 134 Japanese patients with SLE (121 women and 13 men) with a mean age of 41.4 years (range 20–72 years), who presented to our Rheumatic and Connective Tissue Disease Unit, were recruited for the study. All of them fulfilled the American College of Rheumatology criteria for SLE (6). Fifteen patients (11.2%) fulfilled the Sapporo criteria for definite antiphospholipid syndrome (7). Sixty-seven healthy Japanese individuals were included as a control group. The study was conducted in accordance with the Declaration of Helsinki and the principles of good clinical practice. Approval was obtained from the local ethics committee, and written informed consent was obtained from each patient before enrollment.

Polymorphism status in HPA-1, HPA-4, and HPA-6 was determined by polymerase chain reaction–restriction fragment length polymorphism (PCR-RFLP), as previously described (5), with minor modifications. Briefly, 50 ng of genomic DNA was amplified in a total volume of 10 μl containing dNTPs (200 μM each) in a standard buffer with 1.5 mM $MgCl_2$, 0.5 units of DNA *Taq* polymerase, and 10 pmoles of each primer. The gene-specific primer sequences were as follows: for HPA-1, forward 5′-CTTA GCTATTGGGAAGTGGTAGGGCCTGC-3′ and reverse 5′-ACCTCAGATCTTCTGACTCAAGTCCTAACGTC TCTTATT-3′; for HPA-4, forward 5′-CCTGTGG-ACATCTACTACTTGATGGACC-3′ and reverse 5′-GCCAATCCGCAGGTTACTCGTGAGCATT-3′; and for HPA-6, forward 5′-CTGGCTGGCTGGGATCCCAGTG-3′ and reverse 5′-CCCTGCAGTTCTCCTCACCTGAG-3′. PCRs were performed as follows: for HPA-1, 27 cycles of 94°C for 45 seconds, 55°C for 30 seconds, and 72°C for 45 seconds; for HPA-4, 31 cycles of 94°C for 45 seconds, 55°C for 30 seconds, and 72°C for 45 seconds; and for HPA-6, 27 cycles of 94°C for 45 seconds, 55°C for 30 seconds, and 72°C for 45 seconds. After all cycles were completed, a final extension step of 72°C for 7 minutes was performed in all PCRs.

The amplified products (486 bp, 126 bp, and 240 bp for HPA-1, HPA-4, and HPA-6, respectively) were digested by *Msp* I (New England Biolabs, Beverly, MA) at 37°C for 16 hours for HPA-1, *Bsm* I (New England Biolabs) at 65°C for 1 hour for HPA-4, and *Mva* I (Takara Shuzo, Shiga, Japan) at 37°C for 16 hours for HPA-6. RFLP products were resolved in 9% polyacrylamide gels, stained with ethidium bromide, and visualized under ultraviolet light. For HPA-1, two bands of 274 bp and 206 bp were visualized for the A/A homozygous genotype, and 4 bands of 274 bp, 206 bp, 173 bp, and 101 bp were identified for the heterozygous genotype. For HPA-4, a 104-bp band corresponded to the A/A genotype, and a 126-bp band to the B/B genotype. For HPA-6, A/A single band of 240 bp was visualized for the A/A homozygous genotype. Two bands of 165 bp and 75 bp and 3 bands of 240 bp, 165 bp, and 75 bp were identified for the B/B homozygous genotype and the heterozygous genotype, respectively.

All patients were tested for antiphospholipid antibodies (aPL), including anticardiolipin antibodies (aCL) and lupus anticoagulant (LAC). The aCL (IgG, IgM, and IgA) were assayed as previously described (8), and for the detection of LAC the guidelines of the Subcommitte for Standardization of the International Society of Thrombosis and Haemostasis were followed (9).

The records of the patients were reviewed retrospectively, and autoimmune thrombocytopenia, defined as platelet count $<100 \times 10^9$/liter, was detected in 35 patients (26.1%). Transient thrombocytopenia associated with disseminated intravascular coagulation, thrombotic thrombocytopenic purpura, hemophagocytotic syndrome, drug-induced thrombocytopenia, and myelodysplastic syndrome were not considered to be autoimmune thrombocytopenia. Twenty-one patients (15.7%) had a history of thrombotic events. LACs were detected in 43 patients (32.1%) and aCL in 26 (19.4%).

HPA-1 polymorphism was not present in the study population. The A/A genotype was detected in HPA-1 in 100% of SLE patients and healthy individuals, in accordance with the results of a previous study (5).

The HPA-4 A/A genotype was found in 98.3% of SLE patients and in 97% of healthy individuals. The heterozygous

Table 1. Distribution of the HPA-6 genotypes*

Group (n)	A/A genotype	A/B genotype	B/B genotype
Healthy controls (67)	66 (98.5)	1 (1.5)	0 (0)
All SLE patients (134)†	124 (92.5)	10 (7.5)	0 (0)
Patients with thrombocytopenia (35)‡	28 (80)	7 (20)	0 (0)
Patients without thrombocytopenia (99)	96 (97)	3 (3)	0 (0)
Patients with thrombosis (21)	21 (100)	0 (0)	0 (0)
Patients without thrombosis (113)	103 (91.2)	10 (8.8)	0 (0)
Patients with aPL (52)	50 (96.2)	2 (3.8)	0 (0)
Patients without aPL (82)	74 (90.2)	8 (9.8)	0 (0)

* Values are the number (%) of subjects. HPA-6 = human platelet antigen 6; SLE = systemic lupus erythematosus; aPL = antiphospholipid antibody.
† Odds ratio (OR) 5.32 (95% confidence interval [95% CI] 0.66–42.48).
‡ OR 8 (95% CI 1.9–32.9), $P < 0.0028$.

genotype was observed in 2 patients and in 2 controls (1.5% and 3%, respectively), a slightly higher frequency than that previously found by Tanaka et al in 331 random donors (0.3%) (5).

The HPA-6 A/B genotype was found in 7.5% of patients with SLE, compared with 1.5% of healthy controls. There was no significant deviation from Hardy-Weinberg equilibrium in either group. The HPA-6 A/B genotype was more frequently observed in patients with thrombocytopenia than in those without (odds ratio 8, [95% confidence interval 1.94–32.98], $P = 0.0028$). There was no difference in genotype distribution based on the presence or absence of thrombotic events or aPL (Table 1).

The first recognized platelet alloantigen was seen in 1959 in a patient with clinical features of posttransfusion purpura (10). Since then, >20 alloantigens have been described and attributed to different antigen systems. The HPA-6 polymorphism is due to an Arg–Gln variation at position 489. We found the HPA-6 A/B genotype in 5.5% of subjects, a frequency similar to that previously found in Japanese donors (4.8%) (11), and significantly higher than that observed in a Finnish population (0.7%) (12).

The initial aim of our study was to identify a risk factor for thrombosis, apart from the presence of aPL, in patients with SLE. The strong correlation between HPA-1 polymorphism and coronary events (4) drove us to investigate a link between HPA polymorphisms and thrombosis in SLE. In the present study there was no statistically significant difference between the frequency of the HPA-6 A/B genotype in patients and that in healthy controls. None of the HPA polymorphisms investigated in this study were identified as a risk factor for thrombosis in the study population. Interestingly, the HPA-6 A/B genotype occurred significantly more frequently in SLE patients with autoimmune thrombocytopenia than in those without.

Autoimmune thrombocytopenia, one of the most common features of SLE, occurs in 7–30% of patients during the course of the disease, but its pathogenesis is still controversial. One postulated mechanism of platelet destruction in SLE involves the presence of antiplatelet antibodies, mainly directed against the GPIIb-IIIa complex, which bind to circulating platelets and facilitate the clearance of platelets by the reticuloendothelial system (1,13). Alternatively, aPL may interact with platelet phospholipids, leading to platelet destruction by the reticuloendothelial system (14,15)

The significance of antigen polymorphisms in the development of autoimmune thrombocytopenia is far from clear. Polymorphisms in GPIIb-IIIa may potentially promote the production of autoantibodies. Platelet GPIIb-IIIa is the main antigenic target recognized by antiplatelet antibodies in autoimmune thrombocytopenia, and anti–GPIIb-IIIa antibodies have been measured in SLE-associated thrombocytopenia using an indirect monoclonal-specific immobilization of platelet antigens assay (1) or an enzyme-linked immunosorbent assay, which detects peripheral blood B cells secreting IgG anti–GPIIb-IIIa (16). It would be of interest to analyze the association between anti–GPIIb-IIIa and HPA-6 polymorphism. Unfortunately, our study design did not include the detection of antiplatelet antibodies, and neither of these detection methods was performed.

In our thrombocytopenia patients with the HPA-6 A/B genotype, platelet count ranged from 3.2×10^9 to 9.8×10^9/liter, implying that the association between HPA-6 A/B genotype and thrombocytopenia has an immunogenetic impact rather than clinical significance as a predictor of bleeding tendency.

In conclusion, our preliminary findings show that the HPA-6 A/B genotype is a risk factor for autoimmune thrombocytopenia in SLE. Further investigations are needed to clarify the relationship between this polymorphism and thrombocytopenia in SLE.

Supported by grants from the Japanese Ministry of Health, Labor, and Welfare and the Japanese Ministry of Education, Culture, Sports, Science, and Technology.

AUTHOR CONTRIBUTIONS

Dr. Atsumi had full access to all of the data in the study and takes responsibility for the integrity of the data and the accuracy of the data analysis.

Study design. Amengual, Atsumi, Komano, Kataoka, Horita, Yasuda, Koike.

Acquisition of data. Amengual, Atsumi, Komano, Kataoka, Horita, Yasuda, Koike.

Analysis and interpretation of data. Amengual, Atsumi, Komano, Kataoka, Horita, Yasuda, Koike.

Manuscript preparation. Amengual, Atsumi, Komano, Kataoka, Horita, Yasuda, Koike.
Statistical analysis. Amengual, Atsumi.

Olga Amengual, MD, PhD
Tatsuya Atsumi, MD, PhD
Yukiko Komano, MD
Hiroshi Kataoka, MD, PhD
Tetsuya Horita, MD, PhD
Shinsuke Yasuda, MD, PhD
Takao Koike, MD, PhD
Department of Medicine II
Hokkaido University Graduate School of Medicine
Sapporo, Japan

1. Kuwana M, Kaburaki J, Okazaki Y, Miyazaki H, Ikeda Y. Two types of autoantibody-mediated thrombocytopenia in patients with systemic lupus erythematosus. Rheumatology (Oxford) 2006;45: 851–4.
2. Von dem Borne AE, Ouwehand WH. Immunology of platelet disorders. Baillieres Clin Haematol 1989;2:749–81.
3. Goldschmidt-Clermont PJ, Shear WS, Schwartzberg J, Varga CF, Bray PF. Clues to the death of an Olympic champion [letter]. Lancet 1996;347:1833.
4. Walter DH, Schachinger V, Elsner M, Dimmeler S, Zeiher AM. Platelet glycoprotein IIIa polymorphisms and risk of coronary stent thrombosis. Lancet 1997;350:1217–9.
5. Tanaka S, Ohnoki S, Shibata H, Okubo Y, Yamaguchi H, Shibata Y. Gene frequencies of human platelet antigens on glycoprotein IIIa in Japanese. Transfusion 1996;36:813–7.
6. Tan EM, Cohen AS, Fries JF, Masi AT, McShane DJ, Rothfield NF, et al. The 1982 revised criteria for the classification of systemic lupus erythematosus. Arthritis Rheum 1982;25:1271–7.
7. Miyakis S, Lockshin MD, Atsumi T, Branch DW, Brey RL, Cervera R, et al. International consensus statement on an update of the classification criteria for definite antiphospholipid syndrome (APS). J Thromb Haemost 2006;4:295–306.
8. Harris EN, Gharavi AE, Patel SP, Hughes GR. Evaluation of the anti-cardiolipin antibody test: report of an international workshop held 4 April 1986. Clin Exp Immunol 1987;68:215–22.
9. Brandt JT, Triplet DA, Alving B, Scharrer I, on behalf of the Subcommittee on Lupus Anticoagulant/Antiphospholipid Antibody of the Scientific and Standardisation Committee of the ISTH. Criteria for the diagnosis of lupus anticoagulants: an update. Thromb Haemost 1995;74:1185–90.
10. Van Loghem JJ, Dorfmeijer H, Van Hart M, Schreuder F. Serological and genetical studies on a platelet antigen (Zw). Vox Sang 1959;4:161–9.
11. Tanaka S, Taniue A, Nagao N, Tomita T, Ohnoki S, Shibata H, et al. Genotype frequencies of the human platelet antigen, Ca/Tu, in Japanese, determined by a PCR-RFLP method. Vox Sang 1996; 70:40–4.
12. Kekomaki R, Jouhikainen T, Ollikainen J, Westman P, Laes M. A new platelet alloantigen, Tua, on glycoprotein IIIa associated with neonatal alloimmune thrombocytopenia in two families. Br J Haematol 1993;83:306–10.
13. Michel M, Lee K, Piette JC, Fromont P, Schaeffer A, Bierling P, et al. Platelet autoantibodies and lupus-associated thrombocytopenia. Br J Haematol 2002;119:354–8.
14. Harris EN, Asherson RA, Gharavi AE, Morgan SH, Derue G, Hughes GR. Thrombocytopenia in SLE and related autoimmune disorders: association with anticardiolipin antibody. Br J Haematol 1985;59:227–30.
15. Atsumi T, Furukawa S, Amengual O, Koike T. Antiphospholipid antibody associated thrombocytopenia and the paradoxical risk of thrombosis. Lupus 2005;14:499–504.
16. Kuwana M, Okazaki Y, Kaburaki J, Ikeda Y. Detection of circulating B cells secreting platelet-specific autoantibody is useful in the diagnosis of autoimmune thrombocytopenia. Am J Med 2003;114:322–5.

ARTHRITIS & RHEUMATISM
Vol. 56, No. 2, February 2007, pp 393–394
DOI 10.1002/art.22366

EDITORIAL

"Resurrection of Thrombin" in the Pathophysiology of the Antiphospholipid Syndrome

Takao Koike and Tatsuya Atsumi

Antiphospholipid syndrome (APS) is characterized by recurrent thrombosis associated with the persistent presence of antiphospholipid antibodies (aPL) (1). Many of the autoantibodies associated with APS are directed against phospholipid-binding plasma proteins such as β_2-glycoprotein I (β_2GPI) and prothrombin expressed on, or bound to, the surface of vascular endothelial cells, platelets, or other cells.

Beta$_2$-glycoprotein I was first described in 1961 as a component of the β-globulin fraction of human serum (2). However, it was not until the early 1990s that clear evidence emerged of the major role of β_2GPI in the binding of anticardiolipin antibodies to phospholipids in patients with APS. Over the following years, detailed studies have been performed to define its structure and properties. Beta$_2$-glycoprotein I, a 50-kd protein, is a single polypeptide chain composed of 326 amino acid residues with 5 oligosaccharide attachment sites (3). This protein is composed of 5 homologous motifs designated short consensus repeats (SCRs) or sushi domains. Human β_2GPI has been crystallized, and its tertiary structure has revealed a highly glycosylated protein with an elongated fishhook-like arrangement of the globular SCR domains (4,5). Beta$_2$-glycoprotein I has a major phospholipid binding site located in the fifth domain, C^{281}KNKEKKC^{288}, close to the hydrophobic loop.

Recently, great interest has arisen concerning the binding of aPL to endothelial cells or other procoagulant cells and how this binding mediates cell dysfunctions that potentially induce the clinical manifestations of APS. A few years ago, the signal transduction mechanism implicated in the induction of procoagulant substances by aPL was examined. There is now clear evidence that the p38 MAPK pathway of cell activation plays an important role in aPL-mediated cell activation (6–8). Moreover, the role of annexin A2 as a receptor for β_2GPI (9) and the interaction of β_2GPI with different members of the low-density lipoprotein receptor family (10) have been recently reported.

Before this era of cell biology, clinical features of APS were considered as "coagulopathy," and the mechanisms involved in the coagulation cascade abnormality mediated by aPL had been intensively investigated since the early 1980s. Currently, the coagulopathy concept appears to have minor standing within a cluster of reports described in the previous paragraph. However, it is still noted that a significant reduction of in vitro thrombin generation was found in plasma from β_2GPI-null mice, indicating that β_2GPI may play an important role in thrombin generation (11). The in vitro properties of β_2GPI as a natural regulator of coagulation have been proposed in a large number of reports. Beta$_2$-glycoprotein I may act as an anticoagulant by binding to the phospholipids on platelet surfaces and inhibiting the contact pathway. In addition, β_2GPI binds directly to factor XI and inhibits activation of factor XI by thrombin or activated factor XII; this inhibition attenuates thrombin generation (12).

Thrombin, a member of the serine protease family, is a key enzyme in hemostasis. Thrombin is generated from its inactive precursor prothrombin by activated factor X as part of the prothrombinase complex on the surface of activated cells. Thrombin may function as a procoagulant not only by cleaving fibrinogen to fibrin, but also by interacting with protease-activated receptors (PARs) on many types of procoagulant cells and with GPIb-IX-V complex on the surface of platelets, leading to platelet aggregation and activation. On the other hand, thrombin may behave as an anticoagulant upon binding to thrombomodulin to favor activation of protein C. Furthermore, thrombin takes part in the regulation of numerous physiologic and pathophys-

Takao Koike, MD, PhD, Tatsuya Atsumi, MD, PhD: Hokkaido University Graduate School of Medicine, Sapporo, Japan.
Address correspondence and reprint requests to Takao Koike, MD, PhD, Department of Medicine II, Hokkaido University Graduate School of Medicine, N15 W7, Kita-ku, Sapporo 060-8638, Japan. E-mail: tkoike@med.hokudai.ac.jp.
Submitted for publication September 4, 2006; accepted in revised form October 23, 2006.

iologic functions, such as promotion of inflammation, carcinogenesis, angiogenesis, atherosclerosis, and the tissue reparative process (13).

In this issue of *Arthritis & Rheumatism*, Rahgozar et al (14) elegantly demonstrate that β_2GPI is able to bind exosites I and II on thrombin, and that domain V of β_2GPI is essential for this interaction. The interaction between β_2GPI and thrombin may interfere with the coagulation system as well as with many of the biologic functions in which thrombin participates. The significance of β_2GPI binding to thrombin needs further investigation, but direct interaction of β_2GPI with thrombin, one of the most potent enzymes present in the body, opens a new insight into the pathophysiology of the manifestations of APS. It is recognized worldwide that the mechanisms of thrombosis in APS are multifactorial. The direct involvement of thrombin may be a clue to this pluripathologic process.

A second major antigenic target in APS is prothrombin. Most APS patients have anti-β_2GPI antibodies and/or antiprothrombin antibodies. These 2 populations of antibodies are believed to share pathogenic roles in thrombosis in APS. Prothrombin is a precursor of thrombin; thus, the 2 major antigenic players, β_2GPI and prothrombin, encounter each other around the clot formation process.

Rahgozar et al (14) also investigated the effect of monoclonal anti-β_2GPI antibodies in the inhibition of factor XI activation by β_2GPI and thrombin complex, and they show that anti-β_2GPI antibodies enhance this inhibition, leading to a decreased generation of thrombin. It is apparently paradoxical that anti-β_2GPI antibodies enhance one function of the antigen, but this is similar to the effect seen in the β_2GPI, anti-β_2GPI antibodies, and protein C scenario (15). Anti-β_2GPI antibodies enhanced the inhibitory effect of β_2GPI on activated protein C, which proteolyzes activated factor V/activated factor VIII, and reduced thrombin generation. The direct effect of anti-β_2GPI antibodies on thrombin-dependent factor XI activation may, in part, explain why anti-β_2GPI antibodies have lupus anticoagulant activity, but it cannot explain the increased thrombin generation found in APS patients.

In conclusion, Rahgozar et al provide evidence that β_2GPI and thrombin interact directly with each other and that anti-β_2GPI antibodies may modify the "ultimate" generation of thrombin, reminding us of the importance of thrombin, a main player in the era of "coagulopathy," for explaining the formation of clots. The phenomena provide a step forward in the understanding of the etiologic chart of APS. These data have brought thrombin into the center of the chart again, although many details are still far from being elucidated.

REFERENCES

1. Khamashta MA. Hughes syndrome: history. In: Khamashta MA, editor. Hughes syndrome: antiphospholipid syndrome. 2nd ed. London: Springer-Verlag; 2006. p. 3–8.
2. Schultze HE, Heide K, Haput H. Uber ein bisher ubekanntes niedermolekulars β2-Globulin des Humanserums. Naturwissenschaften 1961;48:719.
3. Lozier J, Takahashi N, Putnam FW. Complete amino acid sequence of human plasma β2-glycoprotein I. Proc Natl Acad Sci U S A 1984;81:3640–4.
4. Bouma B, de Groot PG, van den Elsen JM, Ravelli RB, Schouten A, Simmelink MJ, et al. Adhesion mechanism of human β_2-glycoprotein I to phospholipids based on its crystal structure. EMBO J 1999;18:5166–74.
5. Schwarzenbacher R, Zeth K, Diederichs K, Gries A, Kostner GM, Laggner P, et al. Crystal structure of human β2-glycoprotein I: implications for phospholipid binding and the antiphospholipid syndrome. EMBO J 1999;18:6228–39.
6. Bohgaki M, Atsumi T, Yamashita Y, Yasuda S, Sakai Y, Furusaki A, et al. The p38 mitogen-activated protein kinase (MAPK) pathway mediates induction of the tissue factor gene in monocytes stimulated with human monoclonal anti-β_2 glycoprotein I antibodies. Int Immunol 2004;16:1633–41.
7. Vega-Ostertag M, Casper K, Swerlick R, Ferrara D, Harris EN, Pierangeli SS. Involvement of p38 MAPK in the up-regulation of tissue factor on endothelial cells by antiphospholipid antibodies. Arthritis Rheum 2005;52:1545–54.
8. Lopez-Pedrera C, Buendia P, Cuadrado MJ, Siendones E, Aguirre MA, Barbarroja N, et al. Antiphospholipid antibodies from patients with the antiphospholipid syndrome induce monocyte tissue factor expression through the simultaneous activation of NF-κB/Rel proteins via the p38 mitogen-activated protein kinase pathway, and of the MEK-1/ERK pathway. Arthritis Rheum 2006;54:301–11.
9. Zhang J, McCrae KR. Annexin A2 mediates endothelial cell activation by antiphospholipid/anti-β2 glycoprotein I antibodies. Blood 2005;105:1964–9.
10. Pennings MT, van Lummel M, Derksen RH, Urbanus RT, Romijn RA, Lenting PJ, et al. Interaction of β2-glycoprotein I with members of the low density lipoprotein receptor family. J Thromb Haemost 2006;4:1680–90.
11. Sheng Y, Reddel SW, Herzog H, Wang YX, Brighton T, France MP, et al. Impaired thrombin generation in β2-glycoprotein I null mice. J Biol Chem 2001;276:13817–21.
12. Shi T, Iverson GM, Qi JC, Cockerill KA, Linnik MD, Konecny P, et al. β 2-Glycoprotein I binds factor XI and inhibits its activation by thrombin and factor XIIa: loss of inhibition by clipped β 2-glycoprotein I. Proc Natl Acad Sci U S A 2004;101:3939–44.
13. Huntington JA. Molecular recognition mechanisms of thrombin. J Thromb Haemost 2005;3:1861–72.
14. Rahgozar S, Yang Q, Giannakopoulos B, Yan X, Miyakis S, Krilis SA. Beta$_2$-glycoprotein I binds thrombin via exosite I and exosite II: anti-β_2-glycoprotein I antibodies potentiate the inhibitory effect of β_2-glycoprotein I on thrombin-mediated factor XIa generation. Arthritis Rheum 2007;56:605–613.
15. Ieko M, Ichikawa K, Triplett DA, Matsuura E, Atsumi T, Sawada KI, et al. β_2-glycoprotein I is necessary to inhibit protein C activity by monoclonal anticardiolipin antibodies. Arthritis Rheum 1999;42:167–74.

Two weeks after stopping this immunosuppression we applied the monoclonal anti-CD20 antibody rituximab. Two rituximab infusions (375 mg/m^2 IV) plus a single additive dose of 100 mg prednisolone IV at 4-week intervals induced remission of polyarthritis and other symptoms in both cases. The concomitant oral steroid dose could be tapered from 50 mg to 5 mg oral prednisolone/day. FACS analysis of lymphocytes showed depletion of circulating B cells. The patients have remained in remission receiving either MTX or ciclosporin after a follow up period of 6 months.

AOSD is a rare systemic inflammatory disorder of unknown origin. The treatment of AOSD is often difficult. Non-steroidal anti-inflammatory drugs, steroids, and disease modifying antirheumatic drugs have been shown to be effective in the treatment of AOSD. Recently, two case studies reported the successful induction of remission with the interleukin 1 receptor antagonist anakinra in refractory AOSD.[1 2] In addition to the patient reported by Aarntzen *et al*,[1] two of the six patients reported on by Fitzgerald *et al*[2] had been resistant to etanercept treatment. Anakinra rapidly induced remission in these three patients,[1 2] whereas rituximab was effective in both of our TNFα inhibitor (etanercept and infliximab) resistant patients. Concomitant oral prednisolone dosages could be tapered to 5 mg/day and remission maintained with MTX and ciclosporin, respectively during follow up.

The report of Aarntzen *et al*[1] suggests that interleukin 1 rather than TNFα is important in the pathogenesis of AOSD. However, the range of disease manifestations and courses suggests considerable heterogeneity of the disease entity and its pathogenetic background.[3 4] Lymphadenopathy is seen in 65% of patients. Lymph node lesions display distinct patterns. Paracortical hyperplasia may be combined with vascular proliferation, histiocytosis, diffuse T cell infiltration, plasma cells, and B immunoblasts.[5] Lymph node lesions may be reminiscent of malignant T cell lymphoma.[6] However, transition to malignant B cell lymphoma has also been reported.[7] Therefore, B cells might represent another target of successful treatment in AOSD.

Our report suggests that B cell depletion with the monoclonal, chimeric, humanised mouse antibody rituximab may be another possible treatment for refractory AOSD. Our patients did not have any severe adverse events, especially no infections. Edwards *et al*[8] reported a low rate of infections in their trial on rituximab treatment in MTX resistant rheumatoid arthritis. Anakinra treatment has also been reported to be complicated by a low rate of infections (but with apparently less efficacy in rheumatoid arthritis than with TNFα inhibitors). However, some reports of serious infectious complications, such as septicaemia with anakinra treatment, have appeared.[9] To our knowledge this is the first report of the successful induction of remission with rituximab in AOSD. Further studies are needed to determine the place of B cell depletion in AOSD.

Authors' affiliations
K Ahmadi-Simab, P Lamprecht, C Jankowiak, W L Gross, Department of Rheumatology, University Hospital of Schleswig-Holstein, Campus Luebeck, and Rheumaklinik Bad Bramstedt, Ratzeburger Allee 160, 23538 Luebeck, Germany

Correspondence to: Dr K Ahmadi-Simab, Germany; ahmadi@r-on-klinik.de

Accepted 5 January 2006

REFERENCES

1 **Aarntzen EH**, van Riel PL, Barrera P. Refractory adult onset Still's disease and hypersensitivity to non-steroidal anti-inflammatory drugs and cyclo-oxygenase-2 inhibitors: are biological agents the solution? *Ann Rheum Dis* 2005;**64**:1523–4.
2 **Fitzgerald AA**, Leclercq SA, Yan A, Homik JE, Dinarello CA. Rapid responses to anakinra in patients with refractory adult-onset Still's disease. *Arthritis Rheum* 2005;**52**:1794–803.
3 **Chen DY**, Lan JL, Lin FJ, Hsieh TY. Proinflammatory cytokine profiles in sera and pathological tissues of patients with active untreated adult onset Still's disease. *J Rheumatol* 2004;**31**:2189–98.
4 **Chen DY**, Lan JL, Hsieh TY, Chen YH. Clinical manifestations, disease course, and complications of adult-onset Still's disease in Taiwan. *J Formos Med Assoc* 2004;**103**:844–52.
5 **Jeon YK**, Paik JH, Park SS, Park SO, Kim YA, Kim JE, *et al*. Spectrum of lymph node pathology in adult onset Still's disease; analysis of 12 patients with one follow up biopsy. *J Clin Pathol* 2004;**57**:1052–6.
6 **Soy M**, Ergin M, Paydas S. Lymphadenopathy in adult-onset Still's disease mimicking peripheral T-cell lymphoma. *Clin Rheumatol* 2004;**23**:81–2.
7 **Sono H**, Matsuo K, Miyazato H, Sakaguchi M, Matsuda M, Hamada K, *et al*. A case of adult-onset Still's disease complicated by non-Hodgkin's lymphoma. *Lupus* 2000;**9**:468–70.
8 **Edwards JC**, Szczepanski L, Szechinski J, Filipowicz-Sosnowska A, Emery P, Close DR, *et al*. Efficacy of B-cell-targeted therapy with rituximab in patients with rheumatoid arthritis. *N Engl J Med* 2004;**350**:2572–81.
9 **Turesson C**, Riesbeck K. Septicemia with Staphylococcus aureus, beta-hemolytic streptococci group B and G, and Escherichia coli in a patient with rheumatoid arthritis treated with a recombinant human interleukin 1 receptor antagonist (anakinra). *J Rheumatol* 2004;**31**:1876.

Protective effect of pravastatin on vascular endothelium in patients with systemic sclerosis: a pilot study

S Furukawa, S Yasuda, O Amengual, T Horita, T Atsumi, T Koike

Ann Rheum Dis 2006;**65**:1118–1120. doi: 10.1136/ard.2005.046870

In patients with systemic sclerosis (SSc), endothelial cell activation or damage in small vessels is followed by intimal hyperplasia and peripheral ischaemia.[1] Raised levels of plasma von Willebrand factor (vWF), thrombomodulin (TM), and other endothelial/thrombotic markers have been found in patients with SSc[2–5]; vWF is increased in plasma from patients with SSc with diffuse skin involvement and with severe disease, presumably correlating with disease activity.[3] Besides a cholesterol lowering effect, statins exert non-lipid related mechanisms, so-called "pleiotropic effects", which may contribute to reducing risks of cardiovascular events. In this study the effect of a low dose pravastatin on markers of endothelial cell activation/injury and coagulation was investigated in patients with SSc.

This clinical trial was approved by the ethical committee of Hokkaido University Graduate School of Medicine, and all

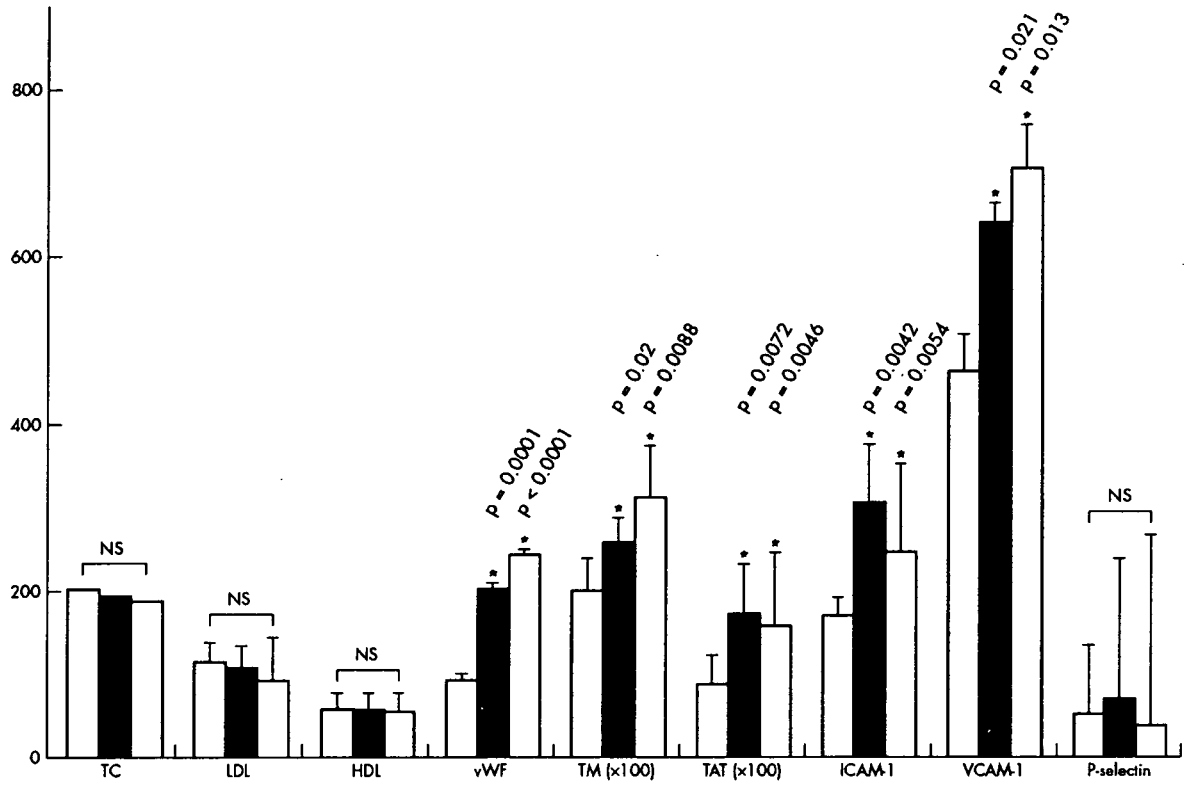

Figure 1 Laboratory data in healthy controls (grey bars), the pravastatin treated group (black bars), and the non-treated group (white bars) before pravastatin treatment. Asterisks indicate that the variable is significantly higher in the treatment group than in the healthy control group. TC, total cholesterol (mg/dl); LDL, low density lipoprotein cholesterol (mg/dl); HDL, high density lipoprotein cholesterol (mg/dl); vWF, von Willebrand factor activity (%); TM, thrombomodulin (fU/ml); TAT, thrombin-antithrombin complex (μg/l); ICAM-1, soluble intercellular adhesion molecule-1 (ng/ml); VCAM-1, soluble vascular cell adhesion molecule-1 (ng/ml); and P-selectin (ng/ml). Error bars indicate standard deviations.

the patients gave their informed consent. The study comprised 18 patients with SSc without hyperlipidaemia (16 women, two men) attending the connective tissue disease clinic of Hokkaido University Hospital (mean (SD) age 52.3 (12.5)). Diagnosis of SSc was based on the American College of Rheumatology criteria.[6] Patients with morphoea were not included in the study.

Nine patients were treated with low dose (10 mg/day) pravastatin for 8 weeks and the other nine patients were not treated. No differences in age, sex, treatment or severity were found between the groups. Three patients from the pravastatin group and four from the non-treatment group were receiving low dose steroids. Ten disease-free subjects matched for age and sex served as healthy controls. Lipid

Table 1 Laboratory data in patients with SSc at days 0 and 56

Data	Pravastatin	Day 0	Day 56	p Value
TC (mmol/l)	(+)	5.00 (0.65)	4.50 (1.10)	NS
	(−)	4.85 (1.35)	4.75 (1.20)	NS
LDL (mmol/l)	(+)	2.80 (0.55)	2.35 (1.00)	NS
	(−)	2.40 (0.60)	2.55 (1.10)	NS
HDL (mmol/l)	(+)	1.60 (0.50)	1.45 (0.35)	NS
	(−)	1.40 (0.35)	1.35 (0.25)	NS
vWF (%)	(+)	201.4 (30.9	163.8 (32.9)	0.0053
	(−)	226.9 (33.5	250.8 (66.1)	NS
TM (fU/ml)	(+)	2.6 (0.6)	2.5 (0.9)	NS
	(−)	3.1 (0.9)	3.2 (0.9)	NS
TAT (mg/l)	(+)	1.7 (0.7)	0.9 (0.3)	0.0052
	(−)	1.7 (1.0)	1.6 (1.3)	NS
ICAM-1 (ng/ml)	(+)	304.6 (90.2)	294.1 (72.0)	NS
	(−)	245.0 (51.1)	253.6 (48.2)	NS
VCAM-1 (ng/ml)	(+)	641.4 (191.4)	691.3 (244.8)	NS
	(−)	702.6 (228.2)	641.4 (191.4)	NS
P-selectin (ng/ml)	(+)	74.1 (37)	75.1 (32)	NS
	(−)	55.6 (35)	56.2 (36)	NS

NS, not significantly different when the values were compared between days 0 and 56.
There were no significant differences in the measures between the pravastatin group and the non-treatment group.
Cholesterol (mmol/l ÷ 0.025084 = mg/dl).

profiles (total cholesterol, low density lipoprotein cholesterol, and high density lipoprotein cholesterol), vWF activity, TM, thrombin-antithrombin complex (TAT), soluble intercellular adhesion molecule-1 (sICAM-1), soluble vascular cell adhesion molecule-1 (sVCAM-1), and P-selectin were measured on days 0 and 56. Fisher's exact test was used for statistical analysis. Values of $p<0.05$ were regarded as significant.

Data before pravastatin treatment were compared between the patient groups and the healthy control group. vWF, TM, TAT, sICAM-1, and sVCAM-1 were significantly increased in the patient groups compared with the healthy controls (fig 1). Before pravastatin administration, no significant difference was found in any measures between the pravastatin group and non-pravastatin group. In the pravastatin group, plasma activity of vWF and TAT on day 56 were significantly reduced compared with those before treatment (table 1). vWF activity in the pravastatin group was significantly lower than in the non-treatment group ($p = 0.024$) on day 56. During the follow up period, low dose pravastatin did not have significant effect on the other measures, including lipid profiles.

vWF is synthesised by endothelial cells and its secretion is triggered by inflammatory/thrombotic mediators, thus establishing it as a marker of endothelial activation/injury. Although TAT is not a generally accepted marker of endothelial injury, it reflects thrombin generation induced by endothelial perturbation. Statins induce an increment in plasminogen activator synthesis and release, a decrease in plasminogen activator inhibitor-1 activity and endothelin-1 expression, and an up regulation of nitric oxide synthase, thus diminishing procoagulant activity and vasoconstriction.[7 8]

In this pilot study, we have shown that low dose pravastatin reduces plasma vWF activity and TAT without affecting lipid profiles and has a protective effect against perturbation of endothelial cells, leading to some beneficial effects in the affected patients.

Authors' affiliations
S Furukawa, S Yasuda, O Amengual, T Horita, T Atsumi, T Koike, Department of Medicine II, Hokkaido University Graduate School of Medicine, Sapporo, Japan

Correspondence to: Dr S Furukawa, sinfuru19680804@hotmail.com

Accepted 5 January 2006

REFERENCES

1 **Kahaleh MB**, Sherer GK, LeRoy EC. Endothelial injury in scleroderma. *J Exp Med* 1979;**149**:1326–35.
2 **Kahaleh MB**, Osborn I, LeRoy EC. Increased factor VIII/von Willebrand factor antigen and von Willebrand factor activity in scleroderma and in Raynaud's phenomenon. *Ann Intern Med* 1981;**94**:482–4.
3 **Herrick AL**, Illingworth K, Blann A, Hay CR, Hollis S, Jayson MI. Von Willebrand factor, thrombomodulin, thromboxane, beta-thromboglobulin and markers of fibrinolysis in primary Raynaud's phenomenon and systemic sclerosis. *Ann Rheum Dis* 1996;**55**:122–7.
4 **Greaves M**, Malia RG, Milford Ward A, Moult J, Holt CM, Lindsey N, *et al*. Elevated von Willebrand factor antigen in systemic sclerosis: relationship to visceral disease. *Br J Rheumatol* 1988;**27**:281–5.
5 **Ames PR**, Lupoli S, Alves J, Atsumi T, Edwards C, Iannaccone L, *et al*. the coagulation/fibrinolysis balance in systemic sclerosis: evidence for a haematological stress syndrome. *Br J Rheumatol* 1997;**36**:1045–50.
6 **ARA**. Association Diagnostic and Therapeutic Criteria Committee. Preliminary criteria for the classification of systemic sclerosis (scleroderma). Subcommittee for scleroderma criteria of the American Rheumatism Association Diagnostic and Therapeutic Criteria Committee. *Arthritis Rheum* 1980;**23**:581–90.
7 **Bourcier T**, Libby P. HMG CoA reductase inhibitors reduce plasminogen activator inhibitor-1 expression by human vascular smooth muscle and endothelial cells. *Arterioscler Thromb Vasc Biol* 2000;**20**:556–62.
8 **Laufs U**, La Fata V, Plutzky J, Liao JK. Upregulation of endothelial nitric oxide synthase by HMG CoA reductase inhibitors. *Circulation* 1998;**97**:1129–35.

CORRECTION

doi: 10.1136/ard.2005.039404corr1

Early menopause, low body mass index, and smoking are independent risk factors for developing giant cell arteritis (Larsson K, Mellström D, Nordborg C, Odén A, Nordberg E. *Ann Rheum Dis* 2006;**65**:529–32.)

We regret that the last author's name was incorrect. It should have been **Nordborg E.**

Additionally, owing to a production problem, which has now been identified, a number of question marks appeared in the abstract between production of the final proof and the printed journal. This has been rectified and readers can now download a corrected copy of the article at http://ard.bmjjournals.com/content/vol65/issue4/

FORTHCOMING EVENTS

2nd European course: Capillaroscopy and Rheumatic Diseases

22–24 September 2006; Genova, Italy
Updating the capillaroscopy technique for diagnosis and follow up and in the rheumatic diseases
Organising secretariat
EDRA SpA, Viale Monza, 133, 20125 Milan, Italy
Tel:+39 02 28172300
Fax: +39 02 91390681
Email: 2ndcapillaroscopy@edraspa.it

Fifth International Congress on Spondylarthropathies

12–14 October 2006; Gent, Belgium
Contact: Medicongress, Waalpoel 28/34, B-9960 Assenede, Belgium
Tel: +32 (0)9 344 39 59
Fax: +32 (0)9 344 40 10
Email: congresses@medicongress.com
Website: http://www.medicongress.com

9th EULAR Post-Graduate Course in Rheumatology

23–27 October 2006; Warsaw, Poland
A course aimed at junior rheumatologists but open to all
20 EULAR bursaries are available
More informations at www.eular.org

OARSI World Congress on Osteoarthritis

7–10 December 2006; Prague Czech Republic
Website: http://www.oarsi.org

Future EULAR congresses

13–16 June 2007; EULAR 2007; Barcelona, Spain
11–14 June 2008; EULAR 2008; Paris, France

Forthcoming events can be found on the website at http:/annrheumdis.com

ARTHRITIS & RHEUMATISM
Vol. 52, No. 1, January 2005, pp 212–218
DOI 10.1002/art.20741

Significance of Valine/Leucine^{247} Polymorphism of β_2-Glycoprotein I in Antiphospholipid Syndrome

Increased Reactivity of Anti–β_2-Glycoprotein I Autoantibodies to the Valine^{247} β_2-Glycoprotein I Variant

Shinsuke Yasuda,[1] Tatsuya Atsumi,[1] Eiji Matsuura,[2] Keiko Kaihara,[2] Daisuke Yamamoto,[3] Kenji Ichikawa,[1] and Takao Koike[1]

Objective. **To clarify the consequences of the valine/leucine polymorphism at position 247 of the β_2-glycoprotein I (β_2GPI) gene in patients with antiphospholipid syndrome (APS), by investigating the correlation between genotypes and the presence of anti-β_2GPI antibody. The reactivity of anti-β_2GPI antibodies was characterized using recombinant Val^{247} and Leu^{247} β_2GPI.**

Methods. **Sixty-five Japanese patients with APS and/or systemic lupus erythematosus who were positive for antiphospholipid antibodies and 61 controls were analyzed for the presence of the Val/Leu^{247} polymorphism of β_2GPI. Polymorphism assignment was determined by polymerase chain reaction followed by restriction enzyme digestion. Recombinant Val^{247} and Leu^{247} β_2GPI were established to compare the reactivity of anti-β_2GPI antibodies to β_2GPI between these variants. The variants were prepared on polyoxygenated plates or cardiolipin-coated plates, and the reactivity of a series of anti-β_2GPI antibodies (immunized anti-human β_2GPI monoclonal antibodies [Cof-19–21] and autoimmune anti-β_2GPI monoclonal antibodies [EY1C8, EY2C9, and TM1G2]) and IgGs purified from patient sera was investigated.**

Results. **A positive correlation between the Val^{247} allele and the presence of anti-β_2GPI antibodies was observed in the patient group. Human monoclonal/polyclonal anti-β_2GPI autoantibodies showed higher binding to recombinant Val^{247} β_2GPI than to Leu^{247} β_2GPI, although no difference in the reactivity of the immunized anti-β_2GPI between these variants was observed. Conformational optimization showed that the replacement of Leu^{247} by Val^{247} led to a significant alteration in the tertiary structure of domain V and/or the domain IV–V interaction.**

Conclusion. **The Val^{247} β_2GPI allele was associated with both a high frequency of anti-β_2GPI antibodies and stronger reactivity with anti-β_2GPI antibodies compared with the Leu^{247} β_2GPI allele, suggesting that the Val^{247} β_2GPI allele may be one of the genetic risk factors for development of APS.**

The antiphospholipid syndrome (APS) is characterized by arterial/venous thrombosis and pregnancy morbidity in the presence of antiphospholipid antibodies (aPL) (1–3). Among the targets of aPL, β_2-glycoprotein I (β_2GPI), which bears epitopes for anticardiolipin antibodies (aCL), has been extensively studied (4–6). APS-related aCL do not recognize free β_2GPI, but do recognize β_2GPI when it is complexed with phospholipids or negatively charged surfaces, by exposure of cryptic epitopes (7) or increment of antigen density (8).

The significance of antigen polymorphism in the production of autoantibodies or the development of autoimmune diseases is now being widely discussed. It is speculated that amino acid substitution in antigens can lead to differences in antigenic epitopes of a given protein. In particular, β_2GPI undergoes conformational

[1]Shinsuke Yasuda, MD, PhD, Tatsuya Atsumi, MD, PhD, Kenji Ichikawa, MD, PhD, Takao Koike, MD, PhD: Hokkaido University Graduate School of Medicine, Sapporo, Japan; [2]Eiji Matsuura, PhD, Keiko Kaihara, PhD: Okayama University Graduate School of Medicine, Okayama, Japan; [3]Daisuke Yamamoto, MD, PhD: Osaka Medical College, Takatsuki, Japan.

Address correspondence and reprint requests to Tatsuya Atsumi, MD, PhD, Medicine II, Hokkaido University Graduate School of Medicine, N15 W7, Kita-ku, Sapporo 060-8638, Japan. E-mail: at3tat@med.hokudai.ac.jp.

Submitted for publication May 10, 2004; accepted in revised form September 27, 2004.

alteration upon interaction with phospholipids (9). β_2GPI polymorphism on or near the phospholipid binding site can affect the binding or production of aCL (anti-β_2GPI autoantibodies), the result being altered development of APS. Polymorphism near the antigenic site, or which leads to alteration of the tertiary structure of the whole molecule, may affect the binding of autoantibodies. Five different gene polymorphisms of β_2GPI attributable to a single-nucleotide mutation have been described: 4 are a single amino acid substitution at positions 88, 247, 306, and 316 (10), and the other is a frameshift mutation associated with β_2GPI deficiency found in the Japanese population (11). In particular, the Val/Leu^{247} polymorphism locates in domain V of β_2GPI, between the phospholipid binding site in domain V and the potential epitopes of anti-β_2GPI antibodies in domain IV, as we reported previously (12). Although anti-β_2GPI antibodies are reported to direct to domain I (13) or domain V (14) as well, it should be considered that a certain polymorphism alters the conformation of the molecule, affecting function or antibody binding at a distant site.

We previously reported that, in a group of British Caucasian subjects, the Val^{247} allele was significantly more frequent in primary APS patients with anti-β_2GPI antibodies than in controls or in primary APS patients without anti-β_2GPI antibodies (15), but the importance of the Val^{247} allele in patients with APS is still controversial. In this study, we analyzed the correlation between the β_2GPI Val^{247} allele and anti-β_2GPI antibodies in the Japanese population. We also investigated the reactivity of anti-β_2GPI antibodies to recombinant Val^{247} β_2GPI and Leu^{247} β_2GPI, using a series of monoclonal anti-β_2GPI antibodies and IgGs purified from sera of patients with APS. Finally, to investigate the difference in anti-β_2GPI binding to those variants, we conformationally optimized to domain V and the domain IV–V complex of β_2GPI variants at position 247, referring the crystal structure of β_2GPI.

PATIENTS AND METHODS

Patients and controls. The study group comprised 65 patients (median age 38 years [range 18–74 years]; 57 women and 8 men) who attended the Hokkaido University Hospital, all of whom were positive for aPL (IgG, IgA, or IgM class aCL, and/or lupus anticoagulant). Thirty-four patients had APS (16 had primary APS, and 18 had secondary APS), and 31 patients did not have APS (24 had systemic lupus erythematosus [SLE], and 7 had other rheumatic diseases). Among all subjects, 19 had a history of arterial thrombosis, and 6 had venous thrombosis. Of the 31 patients with a history of pregnancy, 8 experienced pregnancy complications (some patients had more than 1 manifestation of pregnancy morbidity). Anti-β_2GPI antibodies were detected by enzyme-linked immunosorbent assay (ELISA) as β_2GPI-dependent aCL (16). IgG, IgA, or IgM class β_2GPI-dependent aCL were found in 30, 14, and 21 patients, respectively (some patients had >1 isotype), and 34 patients had at least 1 of those isotypes. Lupus anticoagulant, detected by 3 standard methods described previously (17), was found in 51 patients. The diagnoses of APS and SLE, respectively, were based on the preliminary classification criteria for definite APS (18) and the American College of Rheumatology criteria for the classification of SLE (19). Informed consent was obtained from each patient or control subject. The control group comprised 61 healthy individuals with no history of autoimmune, thrombotic, or notable infectious disease.

Determination of β_2GPI gene polymorphism. Genomic DNA was extracted from peripheral blood mononuclear cells (PBMCs) using a standard phenol–chloroform extraction procedure or the DnaQuick kit (Dainippon, Osaka, Japan). Polymorphism assignment was determined by polymerase chain reaction (PCR) followed by allele-specific restriction enzyme digestion (PCR–restriction fragment length polymorphism) using *Rsa* I (Promega, Southampton, UK) as described previously (15).

Purification of patient IgG. Sera from 11 patients positive for IgG class β_2GPI-dependent aCL were collected. The mean (±SD) titer of aCL IgG from these patients was 29.0 ± 21.5 IgG phospholipid (GPL) units (range 12.4 to >98 GPL units). IgG was purified from these sera using a protein G column and the MAbTrap GII IgG purification kit (Pharmacia Biotech, Freiburg, Germany), as recommended by the manufacturer.

Monoclonal anti-β_2GPI antibodies. Two types of anti-β_2GPI monoclonal antibodies were used. Cof-19, Cof-20, and Cof-21 are mouse monoclonal anti-human β_2GPI antibodies obtained from immunized BALB/c mice, directed to domains V, III, and IV of β_2GPI, respectively. These monoclonal antibodies recognize the native structure of human β_2GPI (12).

EY1C8, EY2C9, and TM1G2 are IgM class autoimmune monoclonal antibodies established from patients with APS (20). These antibodies bind to domain IV of β_2GPI, but only after interaction with solid-phase phospholipids or with a polyoxygenated polystyrene surface. EY1C8 and EY2C9 were established from a patient whose genotype of β_2GPI was heterozygous for Val/Leu^{247}. The genotype of the patient with TM1G2 was not determined.

Preparation of recombinant β_2GPI. As previously reported, genes were expressed in *Spodoptera frugiperda* Sf9 insect cells infected with recombinant baculoviruses (12). A full-length complementary DNA of human β_2GPI coding Val^{247} was originally obtained from Hep-G2 cells (21), and the valine residue was replaced by leucine, using the GeneEditor in vitro Site-Directed Mutagenesis System (Promega, Madison, WI). The sequence of the primers for a mutant Val^{247}→Leu (GTA→TTA) is as follows: 5′-GCATCTTGTAAATTACCTGTGAAAAAAG-3′. A DNA sequence of the mutant was verified by analysis using ABI Prism model 310 (PE Applied Biosystems, Foster City, CA).

Binding assays of monoclonal anti-β_2GPI antibodies and purified IgGs to the recombinant β_2GPI (cardiolipin-coated plate). The reactivity of a series of monoclonal anti-β_2GPI antibodies and IgG fractions (purified from the sera of APS patients positive for IgG class anti-β_2GPI) against 2 β_2GPI variants was investigated using an ELISA. ELISAs were performed using a cardiolipin-coated plate as previously reported (16) but with a slight modification. Briefly, the wells of Sumilon Type S microtiter plates (Sumitomo Bakelite, Tokyo, Japan) were filled with 30 μl of 50 μg/ml cardiolipin (Sigma, St. Louis, MO) and dried overnight at 4°C. After blocking with 2% gelatin in phosphate buffered saline (PBS) for 2 hours and washing 3 times with 0.05% PBS–Tween, 50 μl of 10 μg/ml recombinant β_2GPI and controls were distributed and incubated for 30 minutes at room temperature. Wells were filled with 50 μl of serial dilutions of monoclonal antibodies (Cof-19–21, EY1C8 and EY2C9, and TM1G2) or purified patient IgG (100 μg/ml), followed by incubation for 30 minutes at room temperature. After washing 3 times, 50 μl of alkaline phosphatase–conjugated anti-mouse IgG (1:3,000), anti-human IgM (1:1,000), or anti-human IgG (1:6,000) was distributed and incubated for 1 hour at room temperature. The plates were washed 4 times, and 100 μl of 1 mg/ml *p*-nitrophenyl phosphate disodium (Sigma) in 1*M* diethanolamine buffer (pH 9.8) was distributed. Optical density (OD) was read at 405 nm, with reference at 620 nm. One percent fatty acid–free bovine serum albumin (BSA) (A-6003; Sigma)–PBS was used as sample diluent and control.

Binding assays of monoclonal anti-β_2GPI antibodies to recombinant β_2GPI (polyoxygenated plate). Anti-β_2GPI antibody detection assay using polyoxygenated plates was performed as previously reported (22), with minor modifications. Briefly, the wells of polyoxygenated MaxiSorp microtiter plates (Nalge Nunc International, Roskilde, Denmark) were coated with 50 μl of 1 μg/ml recombinant β_2GPI in PBS and incubated overnight at 4°C. After blocking with 3% gelatin–PBS at 37°C for 1 hour and washing 3 times with PBS–Tween, 50 μl of monoclonal antibodies, diluted with 1% BSA–PBS, were distributed and incubated for 1 hour at room temperature. The following steps were taken, in a similar manner.

Conformational optimization of domain V and the domain IV–V complex in human β_2GPI variants at position 247. A conformation of domain V in the valine variant at position 247 was first constructed from the crystal structure of the leucine variant (implemented in Protein Data Bank: 1C1Z) (23). Replacement of leucine by valine at position 247 was performed using the Quanta system (Molecular Simulations, San Diego, CA), and the model was optimized by 500 cycles of energy minimization by the CHARMm program (24), with hydrophilic hydrogen atoms and TIP3 water molecules (25). Molecular dynamics simulation (5 psec) of the model was then performed with 0.002 psec time steps. The cutoff distance for nonbonded interactions was set to 15Å, and the dielectric constant was 1.0. A nonbonded pair list was updated every 10 steps. The most stable structure of each domain in the dynamics iterations was then optimized by 500 cycles of energy minimization. The final structures of domain V consisted of 2,616 atoms, including 603 TIP3 water molecules, and had a total energy of -1.63×10^4 kcal/mole with a root-mean-square force of 0.869 kcal/mole.

Molecular models of a domain IV–V complex (leucine and valine variants at position 247) were further constructed by considering the location of the oligosaccharide attachment site in domain IV, the location of epitopic regions of the Cof-8 and Cof-20 monoclonal antibodies, the junction between domains IV and V, and molecular surface charges of both domains. These models were again optimized by molecular dynamics simulation and by energy minimization as described above. The final structures of the complex in the leucine and valine variants consisted of 3,773 and 3,778 atoms, respectively, including hydrophilic hydrogen atoms and 806 and 808 TIP3 water molecules, respectively, and had total energy of -2.07×104 and -2.03×104 kcal/mole with a root-mean-square force of 0.985 and 0.979 kcal/mole, respectively.

Statistical analysis. Correlations between the allele frequencies and clinical features such as the positiveness of β_2GPI-dependent aCL were expressed as odds ratios (ORs) and 95% confidence intervals (95% CIs). *P* values were determined by chi-square test with Yates' correction. *P* values less than or equal to 0.05 were considered significant.

RESULTS

Val/Leu^{247} polymorphism of β_2GPI and the presence of β_2GPI-dependent aCL. As shown in Table 1, the Leu^{247} allele was dominant in the population of healthy Japanese individuals, compared with Caucasians, which is consistent with a previous report (26). Japanese patients with anti-β_2GPI had a significantly increased frequency of the Val^{247} allele, compared with Japanese patients without anti-β_2GPI ($P = 0.0107$) or Japanese controls ($P = 0.0209$).

The binding of autoimmune anti-β_2GPI to recombinant Val^{247} and Leu^{247} β_2GPI. Representative binding curves using cardiolipin-coated plates and polyoxygenated plates are shown in Figure 1. Regardless of the type of plates, Cof-20 bound equally to valine and leucine variants of β_2GPI (Figures 1a and c), in any concentration of Cof-20. The binding curves of Cof-19 and Cof-21 were similar to that of Cof-20 (results not

Table 1. Frequency of the Val^{247} allele of β_2GPI in patients with APS*

Group	Japanese	British Caucasians
Patients with anti-β_2GPI	23/68 (33.8)†	48/56 (85.7)‡
Patients without anti-β_2GPI	9/62 (14.5)	39/58 (67.2)
Controls	23/122 (18.9)	55/78 (70.5)

* Values are the number (%). β_2GPI = β_2-glycoprotein I; APS = antiphospholipid syndrome.
† $P = 0.0107$ versus patients without anti-β_2GPI (odds ratio [OR] 3.01, 95% confidence interval [95% CI] 1.26–7.16), and $P = 0.0209$ versus controls, by chi-square test (OR 2.15, 95% CI 1.09–4.23).
‡ $P = 0.204$ versus patients without anti-β_2GPI (OR 2.92, 95% CI 1.16–7.39), and $P = 0.0396$ versus controls, by chi-square test (OR 2.51, 95% CI 1.03–6.13).

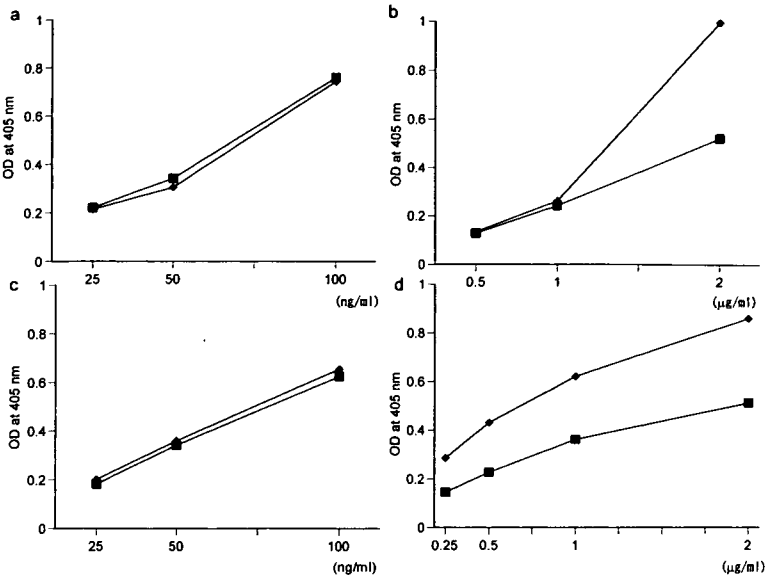

Figure 1. Representative binding curves of monoclonal anti-β_2-glycoprotein I (anti-β_2GPI) antibodies to recombinant valine/leucine^{247} β_2GPI. **a,** Binding curve of Cof-20 using cardiolipin-coated plate. **b,** Binding curve of EY2C9 using cardiolipin-coated plate. **c,** Binding curve of Cof-20 using polyoxygenated plate. **d,** Binding curve of EY2C9 using polyoxygenated plate. Binding to Val^{247} β_2GPI and Leu^{247} β_2GPI are indicated with diamonds and squares, respectively. OD = optical density.

shown). In contrast, EY2C9 showed stronger binding to Val^{247} β_2GPI than to Leu^{247} β_2GPI (Figures 1b and d). EY1C8 and TM1G2 also showed stronger binding to Val^{247} β_2GPI. Figure 2a shows the binding of the monoclonal antibodies, on cardiolipin-coated plates, in the following concentrations: for Cof-19–21, 100 ng/ml;

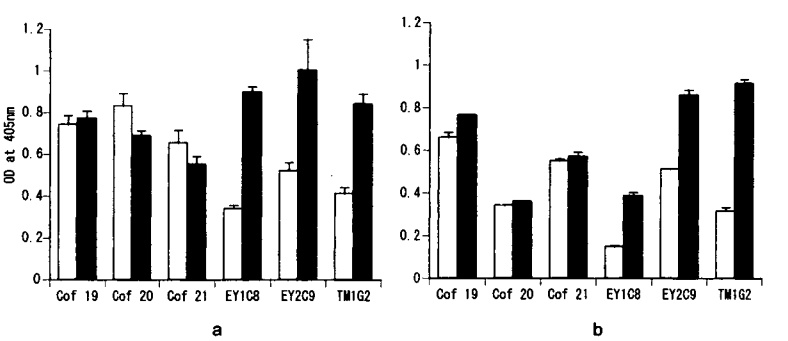

Figure 2. Reactivity of anti-β_2-glycoprotein I (anti-β_2GPI) antibodies to β_2GPI variants. **a,** The binding of monoclonal anti-β_2GPI antibodies to the recombinant valine/leucine^{247} β_2GPI was investigated using enzyme-linked immunosorbent assay (ELISA) on cardiolipin-coated plates. Concentrations of antigens and antibodies were as follows: for recombinant β_2GPI, 10 μg/ml; for Cof-19–21, 100 ng/ml; for EY1C8 and EY2C9, 2 μg/ml; for TM1G2, 5 μg/ml. **b,** The binding of monoclonal anti-β_2GPI antibodies to the recombinant Val/Leu^{247} β_2GPI was investigated using ELISA on polyoxygenated plates. Concentrations of antigens and antibodies were as follows: for recombinant β_2GPI, 1 μg/ml; for Cof-19–21, 50 ng/ml; for EY1C8 and EY2C9, 2 μg/ml; for TM1G2, 5 μg/ml. Results were presented as the optical density (OD) at 405 nm. Open columns indicate binding activity to Leu^{247} β_2GPI, and solid columns indicate binding activity to Val^{247} β_2GPI. Bars show the mean and SD.

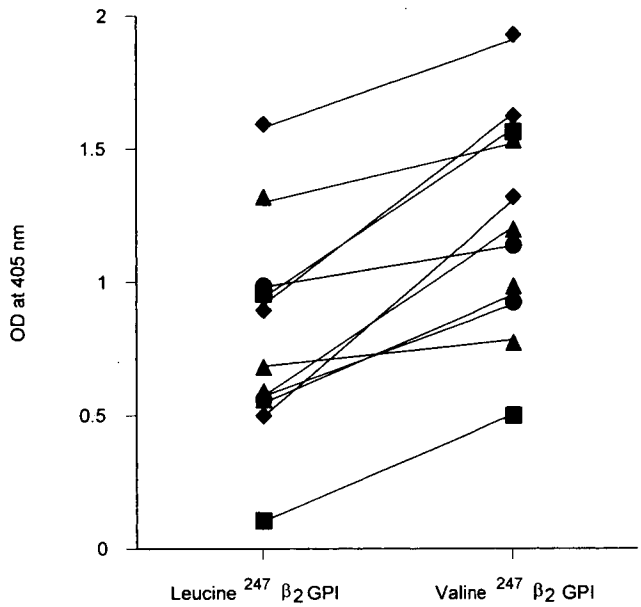

Figure 3. Reactivity of purified IgG from patients (100 μg/ml) to recombinant Val/Leu^{247} β_2-glycoprotein I (β_2GPI) (10 μg/ml), presented as the optical density (OD) at 405 nm. Squares, circles, and triangles indicate patients homozygous for the Leu^{247} allele, homozygous for the Val^{247} allele, and heterozygous for the Val/Leu^{247} allele, respectively. Diamonds indicate patients whose genotypes were not available.

for EY1C8 and EY2C9, 1 μg/ml; and for TM1G2, 2.5μg/ml. In contrast with the close reactivity of Cof-19, Cof-20, and Cof-21 between Val^{247} β_2GPI and Leu^{247} β_2GPI, autoimmune monoclonal antibodies (EY1C8, EY2C9, and TM1G2) showed higher binding to Val^{247} β_2GPI than to Leu^{247} β_2GPI. The autoimmune monoclonal antibodies also showed a higher binding to Val^{247} β_2GPI directly coated on polyoxygenated plates (Figure 2b). IgG in sera collected from 11 patients (100 μg/ml) also showed higher binding to Val^{247} β_2GPI than to Leu^{247} β_2GPI on cardiolipin-coated plates, regardless of the patients' genotypes (Figure 3).

Conformational alteration by leucine replacement by valine at position 247. Each domain V conformation in 2 variants at position 247 is shown in Figure 4a. The root-mean-square deviations for matching backbone atoms and equivalent atoms in the leucine and valine variants were 0.76 and 1.11 Å, respectively. The largest shift was observed at Val^{303}, one of the residues located on the backbone neighboring position 247. The shift seemed to be caused by weak flexibility of side chains consisting of Val^{247}, Pro^{248}, and Val^{249} and the electrostatic interactions between Lys^{250}, Lys^{251}, Glu^{307}, and Lys^{308}.

The molecular models of the IV–V complex in leucine and valine variants are shown in Figure 4b. The root-mean-square deviations for matching these backbone atoms and equivalent atoms were 1.72 and 2.03 Å, respectively. Electrostatic interactions and hydrogen bonds between Asp^{193} and Lys^{246}/Lys^{250}, Asp^{222} and Lys^{305}, and Glu^{228} and Lys^{308} appeared in the IV–V complex, but the interaction between Glu^{228} and Lys^{308} was disrupted by the leucine replacement by valine, because direction of the Lys^{308} side chain was significantly changed in the complex. As a result, Trp^{235} of domain IV, located on the contact surface with domain V, was slightly shifted.

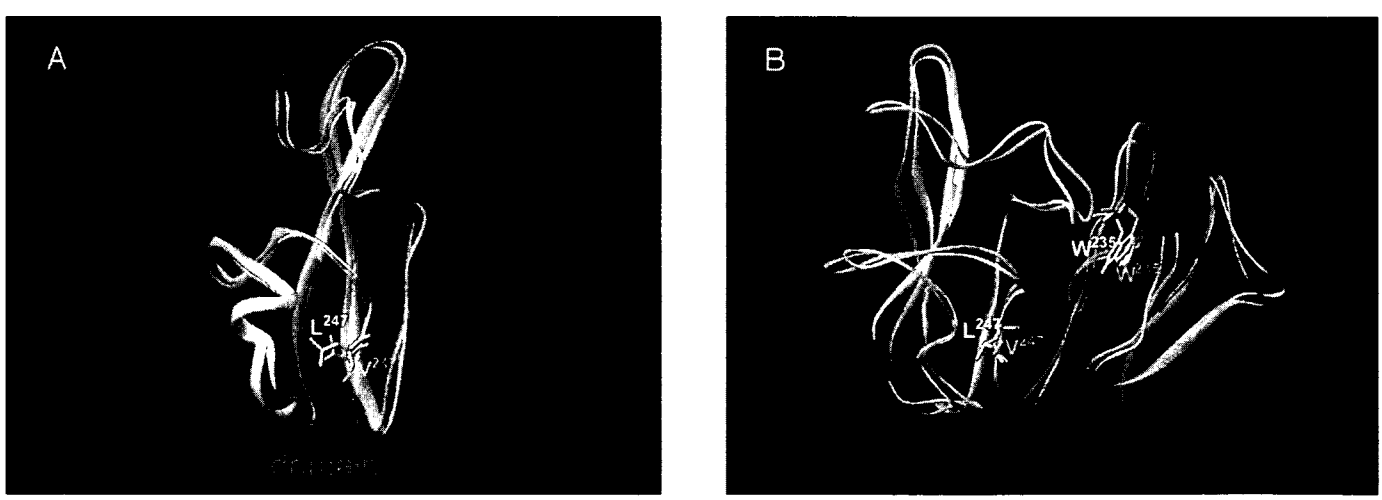

Figure 4. Conformational alterations in domain V (**A**) and in the domain IV–V complex (**B**), replacing leucine by valine at position 247. Structure of the valine (light blue) and leucine (white) variants was shown by a ribbon representation with the secondary structure.

DISCUSSION

This study shows the positive correlation between the Val^{247} β_2GPI allele and anti-β_2GPI antibody production in a Japanese population, confirming the correlation observed in a British Caucasian population in our previous report (15). A positive correlation between the Val^{247} allele and the presence of anti-β_2GPI antibodies was also reported in Asian American (26) and Mexican patients (27). However, this correlation was not observed in other American populations (26) or in patients with thrombosis or pregnancy complications in the UK (28). This discrepancy may be the result of the difference in the frequency of the Val^{247} allele among races, or the difference in the background of investigated patients. Another possibility is that the relationship between the Val^{247} allele and thrombosis in Caucasians may be controversial due to underpowered studies or to differences in the procedure used to detect anti-β_2GPI antibodies. Methods for the detection of anti-β_2GPI antibodies differ among laboratories. For example, cardiolipin-coated plates or oxygenated plates are used in some methods, whereas unoxygenated plates are used in others. In addition, bovine β_2GPI is used instead of human β_2GPI in some assays. The antibodies used for standardization also differ, although monoclonal antibodies such as EY2C9 and HCAL (29) have been proposed as international standards of calibration materials.

β_2GPI is a major target antigen for aCL, and, according to our previous investigation, B cell epitopes reside in domain IV and are considered to be cryptic and to appear only when β_2GPI interacts with negatively charged surfaces such as cardiolipin, phosphatidylserine, or polyoxygenated polystyrene surface (7), although other studies indicate that the B cell epitopes are located on domain I (13) or domain V (14). According to another interpretation for the specificity of aCL, increment of the local antigen density on the negatively charged surface also contributes to anti-β_2GPI detection in ELISA (8,30). Studies on the crystal structure of human β_2GPI revealed that the lysine-rich site and an extended C-terminal loop region on domain V are crucial for phospholipid binding. Position 247 is located at the N-terminal side of domain V, and, around this position, Lys^{242}, Ala^{243}, and Ser^{244} were suggested to play a role in the interaction between domains IV and V (9,23,31).

Although the Val/Leu^{247} polymorphism may not be very critical for the autoantibody binding, the amino acid substitution at this point was revealed to affect the affinity of monoclonal aCL established from patients with APS and that of purified IgG from patients positive for β_2GPI-dependent aCL. We conformationally optimized to domain V and the domain IV–V complex of β_2GPI variants at position 247, referring the crystal structure of β_2GPI. IgG aCL was screened using the standardized aCL ELISA, in which both the Leu^{247} and the Val^{247} allele of β_2GPI are contained as antigen. Although biochemical characteristics and structure are similar between valine and leucine, the replacement of Leu^{247} by Val^{247} leads to a significant alteration in the tertiary structure of domain V and/or the domain IV–V interaction (Figure 4). It is likely that the structural alteration affects the affinity between anti-β_2GPI autoantibodies and the epitope(s) present on its molecule. One explanation for this phenomenon is that this β_2GPI polymorphism affects the electrostatic interaction between domain IV and domain V or the protein–protein interaction, resulting in differences in the accessibility of the recognition site by the autoantibodies, or the local density of β_2GPI.

Another possible explanation of the correlation between the Val/Leu^{247} polymorphism of β_2GPI and anti-β_2GPI antibodies is T cell reactivity. Ito et al (32) investigated T cell epitopes of patients with anti-β_2GPI autoantibodies by stimulating patients' PBMCs with a peptide library that covers the β_2GPI sequence. Four of 7 established CD4+ T cell clones reacted to peptide fragments that include amino acid position 244–264, then position 247 is included among the candidate epitopes. Arai et al (33) found preferred recognition of peptide position 276–290 by T cell clones from patients with APS. They also found high reactivity to peptide 247–261 in one patient. We speculate that a small alteration in the conformation arising from the valine/leucine substitution at position 247 may affect the susceptibility to generate autoreactive T cell clones in patients with APS.

Our results in this study indicate that the Val/Leu^{247} polymorphism affects the antigenicity of β_2GPI for anti-β_2GPI autoantibodies, and that the Val^{247} allele can be a risk factor for having autoantibodies against this molecule. Therefore, the Val/Leu^{247} variation of β_2GPI may be crucial for autoimmune reactivity against β_2GPI. We further show the significance of the Val/Leu^{247} polymorphism of β_2GPI in the strength of the binding between β_2GPI and anti-β_2GPI autoantibodies. The significance of antigen polymorphisms in the production of autoantibodies or in the development of autoimmune diseases is not well understood. To our knowledge, this report is the first to present a genetic polymorphism of